

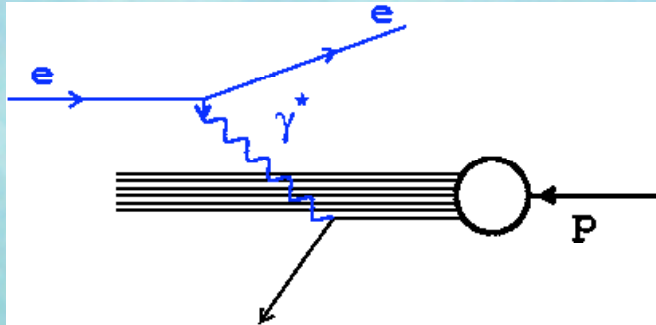
Diffraction at HERA



Henri Kowalski

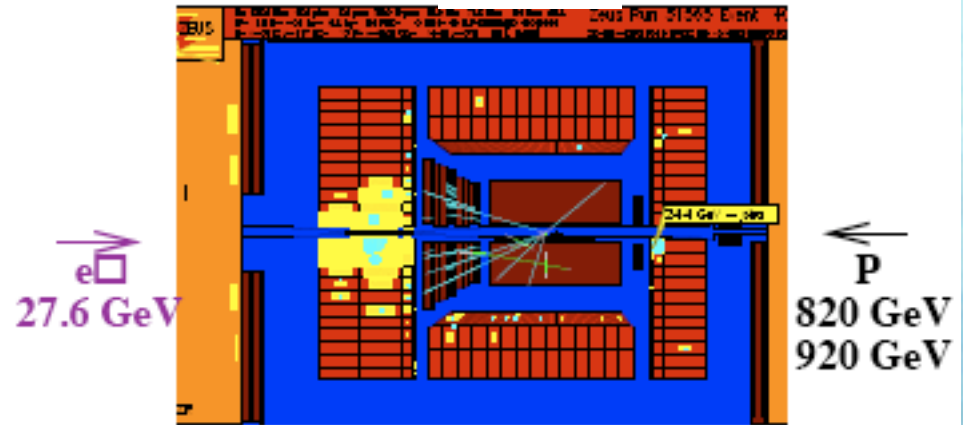
WE- Hereus Summerschool on Diffraction and EM
Heidelberg
5th of September 2011

Non-Diffractive Scattering



Surprise of HERA

ZEUS



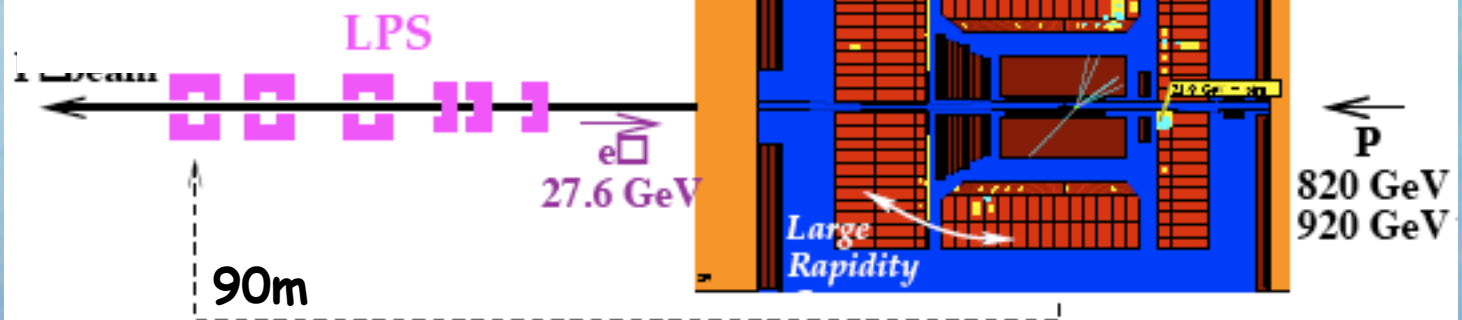
Diffractive Scattering

expectation before HERA

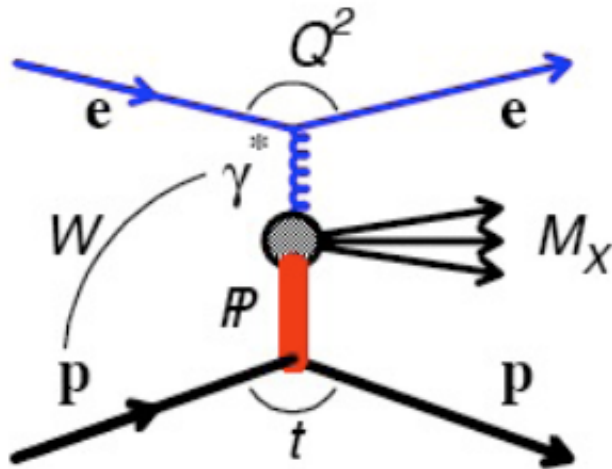
~ 0.01%

seen ~20% at $Q^2 = 4 \text{ GeV}^2$

~10% at $Q^2 = 20 \text{ GeV}^2$



Diffractive Reactions in DIS



Rapidity Gaps

$$\Delta Y = \ln(1/x_{IP}) \sim \ln(W^2/M_X^2) \approx \Delta \eta$$

Forward protons
with $x_L = 1 - x_{IP} > 95\%$
 $x_L \sim$ longitudinal
fraction of proton
momentum

Q^2 - virtuality of the incoming photon

W - CMS energy of the incoming photon-proton system

x - $\approx Q^2 / W^2$

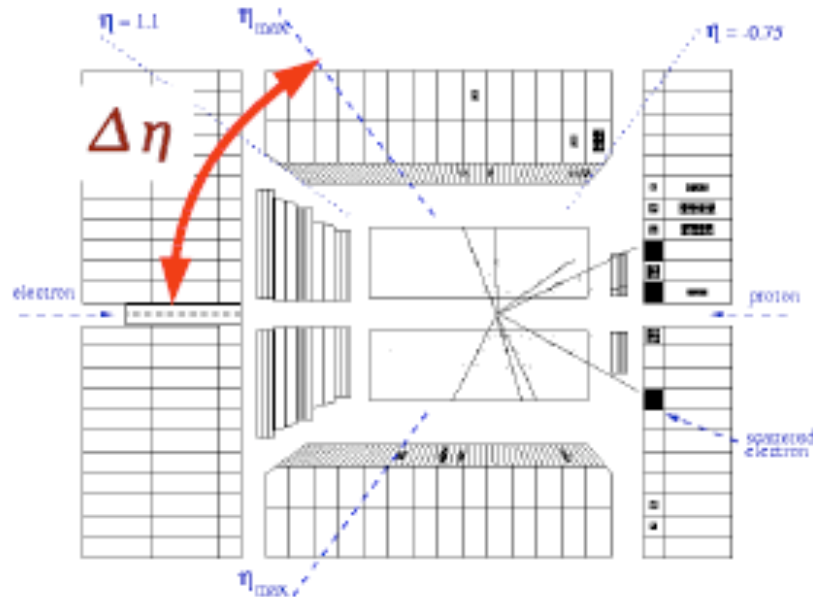
M_X - invariant mass of all particles seen in the detector

t - momentum transfer to the diffractively scattered proton

$$\beta = Q^2 / (Q^2 + M^2)$$

$$x_{IP} = (Q^2 + M^2) / (W^2 + M^2)$$

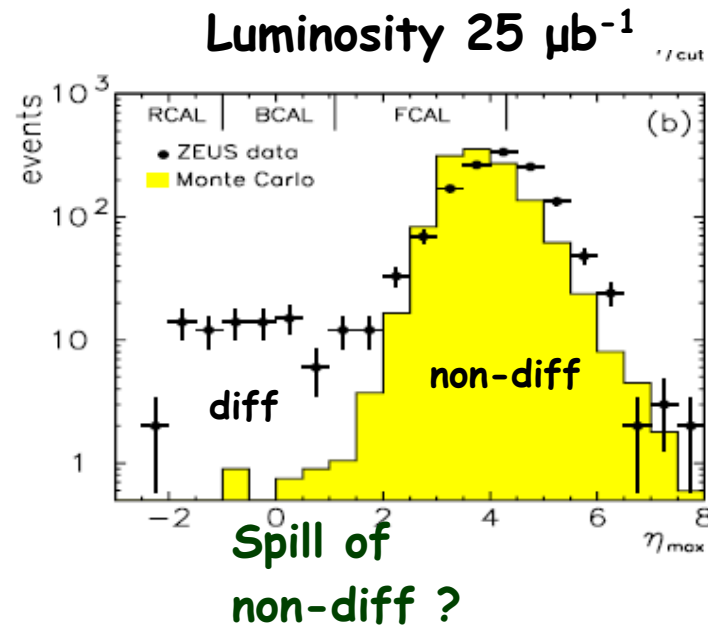
Rapidity Gap Selection



Select diffractive events by requirement:
No energy deposition in some area of the detector
- η_{max} cut

no energy means no cluster with > 400 MeV
note: noise $O(100)$ MeV per cell

ZEUS Collaboration; M.Derrick et al.
Observation of Events with a Large Rapidity Gap in Deep Inelastic Scattering at HERA
DESY 93-093 (July 1993)
Physics Letters B 315 (1993) 481-493



Shape of MC ?
Shifts of MC ?

First diffractive signal seen in DIS

Measurement of the Diffractive Cross Section in Deep Inelastic Scattering using ZEUS 1994 Data DESY 98-084 (July 1998) as a function of W and M_{ν}

The European Physical Journal C 66 (1999) 43-66

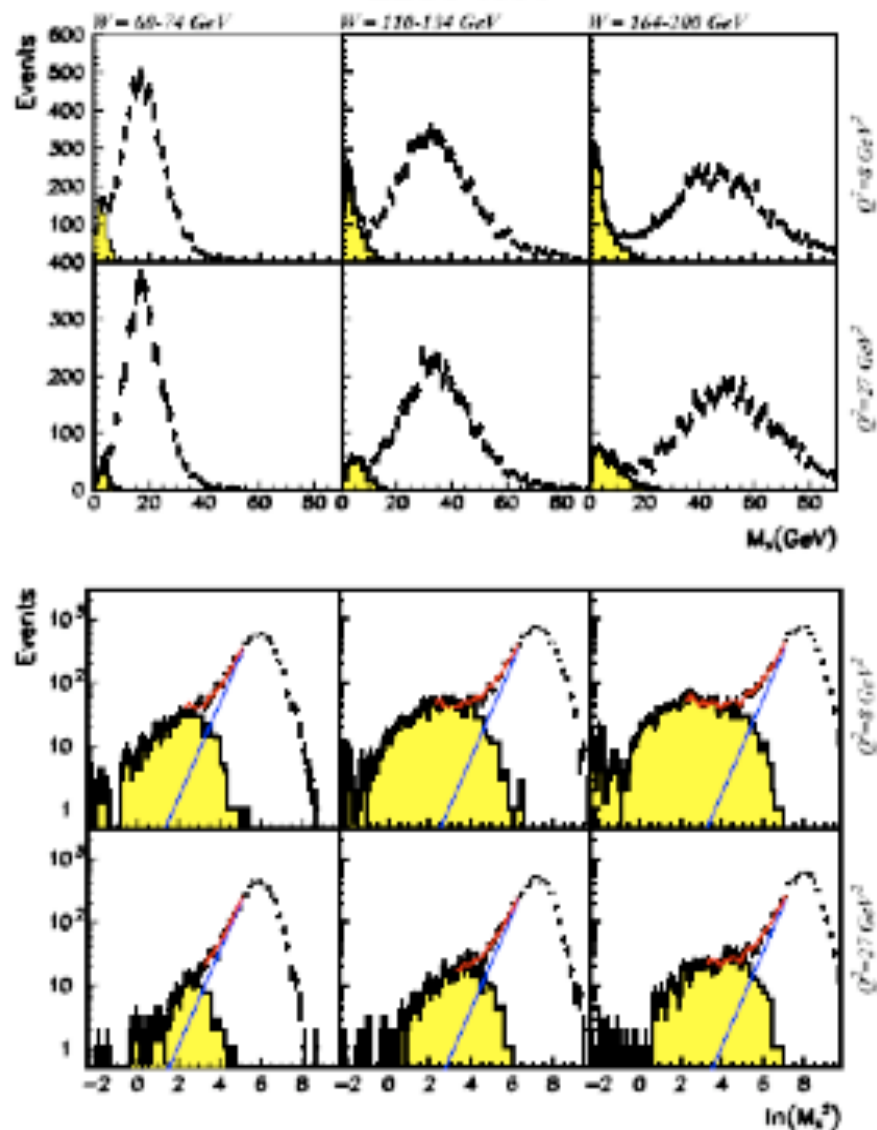


Fig. 1. Reaction $\gamma^*p \rightarrow X + \text{anything}$, where X is the system observed in the detector. *Top:* Distributions of M_X , the corrected mass of the system X . The distributions are not corrected for acceptance effects. The shaded histograms show the distributions of events with $\eta_{\text{max}} < 1.5$. *Bottom:* Same distributions as above presented in terms of $\ln M_X^2$. The straight lines give the nondiffractive contributions as obtained from the fits. The upper curves show the fit results for the sum of the diffractive and nondiffractive contributions

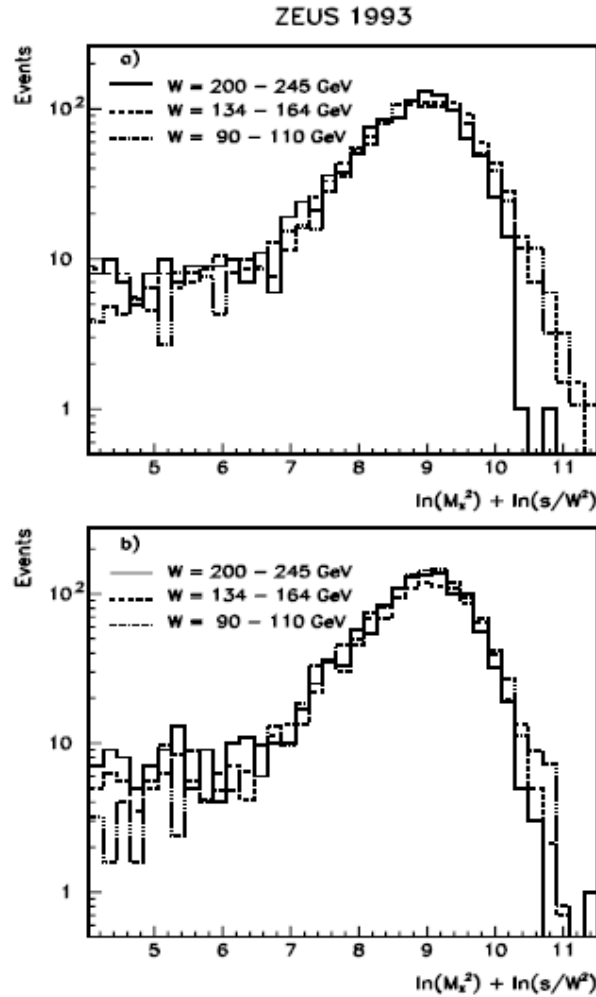
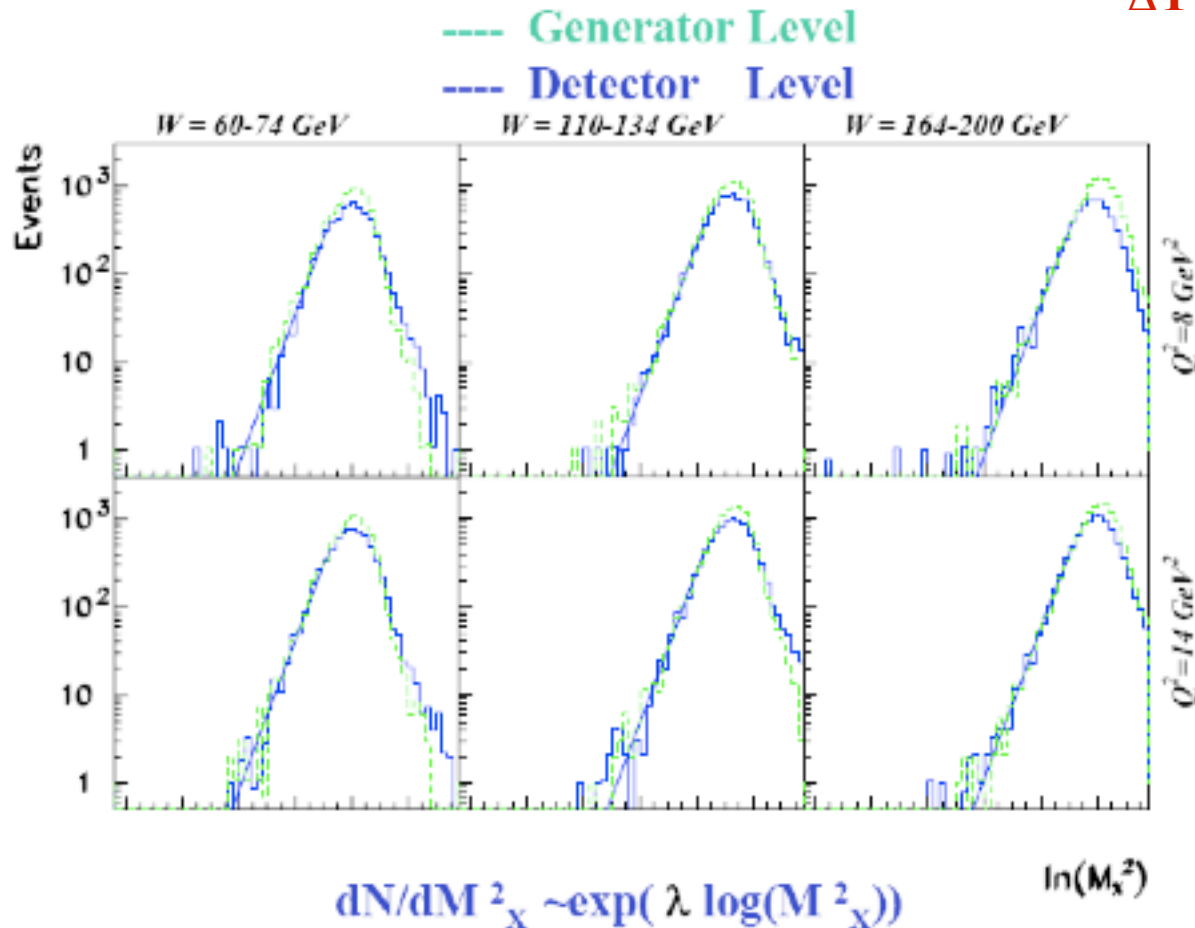


Figure 8: Distributions of $\ln M_X^2 + \ln(s/W^2)$ for the W intervals 90 - 110 GeV (dotted), 134 - 164 GeV (dashed), 200 - 245 GeV (solid) ($\ln W^2 = 9.0 - 9.4, 9.8 - 10.2, 10.6 - 11.0$) at a) $Q^2 = 14 \text{ GeV}^2$ and b) 31 GeV^2 . Here M_X is the corrected mass; the distributions are the measured ones, not corrected for acceptance effects. For each Q^2 the three distributions were normalized to the same number of events.

Non-diff MC (Ariadne) exponentially suppressed RG

$$\Delta Y = \ln(W/M_X)^2$$

$$\Delta Y = \ln(1/x_{IP}) \quad ?$$



In MC λ independent of Q^2 and W^2

$\lambda \sim 2$ in MC

$\lambda \sim 1.7$ in data

→ Watch
the Monte Carlos

Probability to see a gap ΔY in an non-diff event - $\exp(-\lambda\Delta Y)$

Physical interpretation of the Gap Suppression Coef. $\lambda \sim 1.7$

Feynman (~1970): λ depends on the quantum numbers carried by the gap

Photon – Hadron
Interactions,
lecture 52

$\lambda = 2$ for the exchange of pion q.n.

$= 1$ for the exchange of rho q.n.

$= 0$ for the exchange of pomeron q.n.

\Leftrightarrow Regge

\Leftrightarrow phenomenology

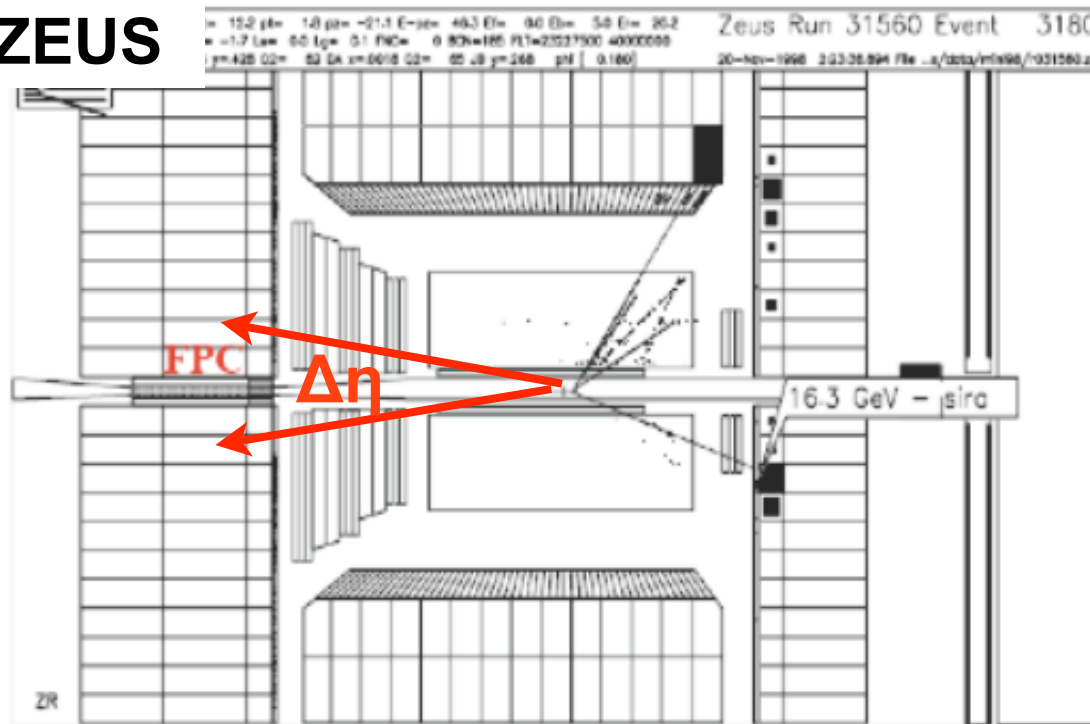
In the Longitudinal Phase Space Model

λ – particle multiplicity per unit of rapidity
cluster

Diffractive Signatures

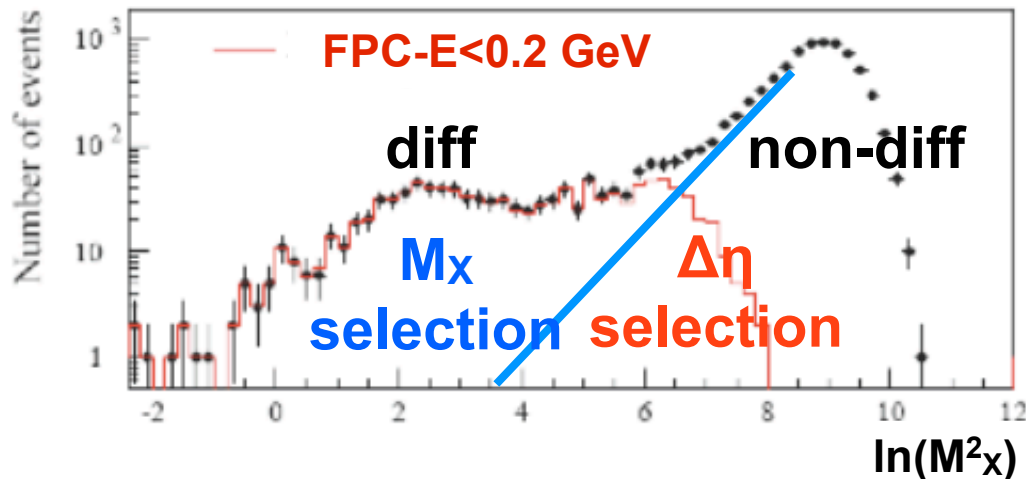
ZEUS

Large
Rapidity
Gap - $\Delta\eta$
selection



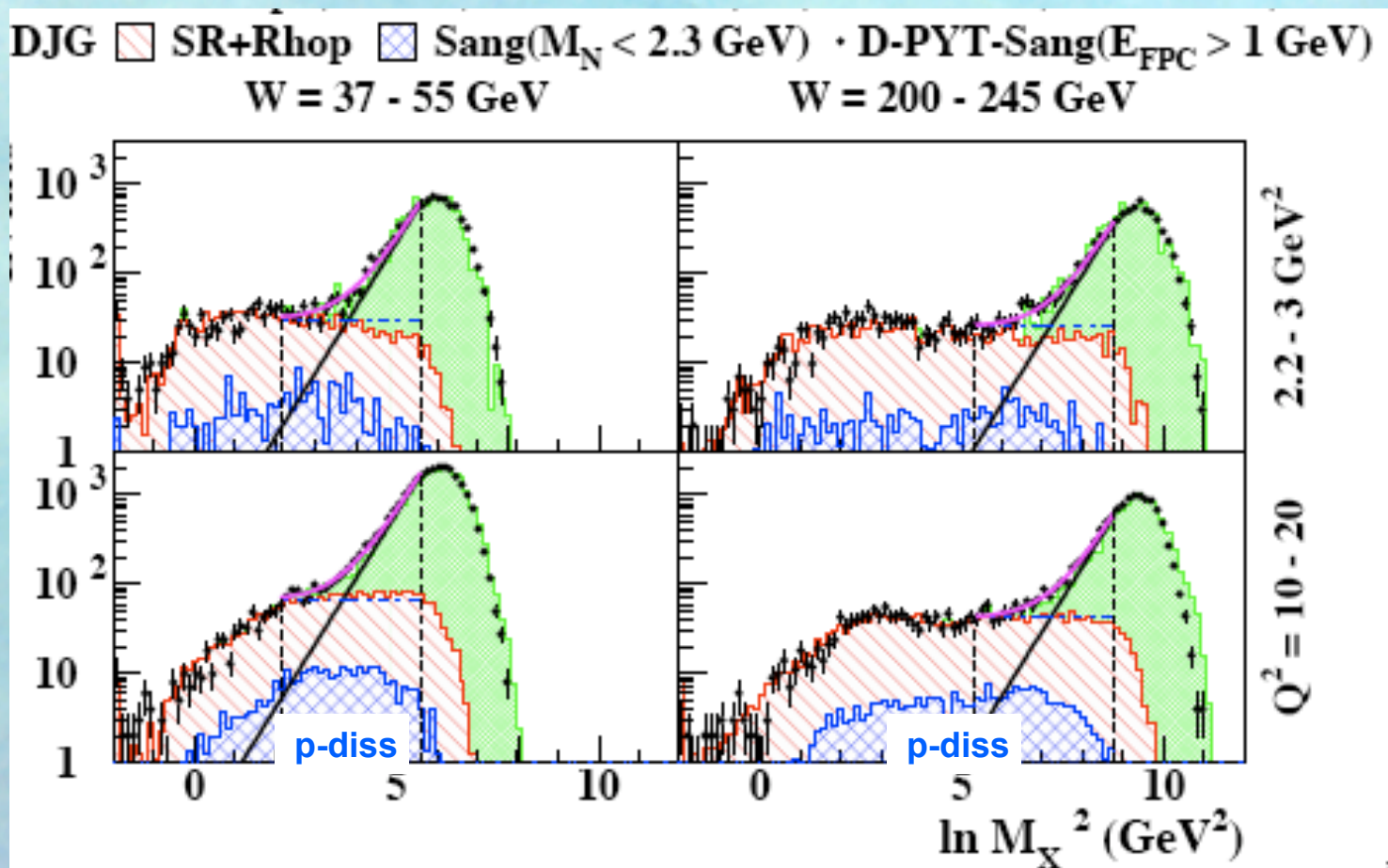
Accidental
LRG ?

M_X Method:
selection of
exponentially
nonsuppressed
RG



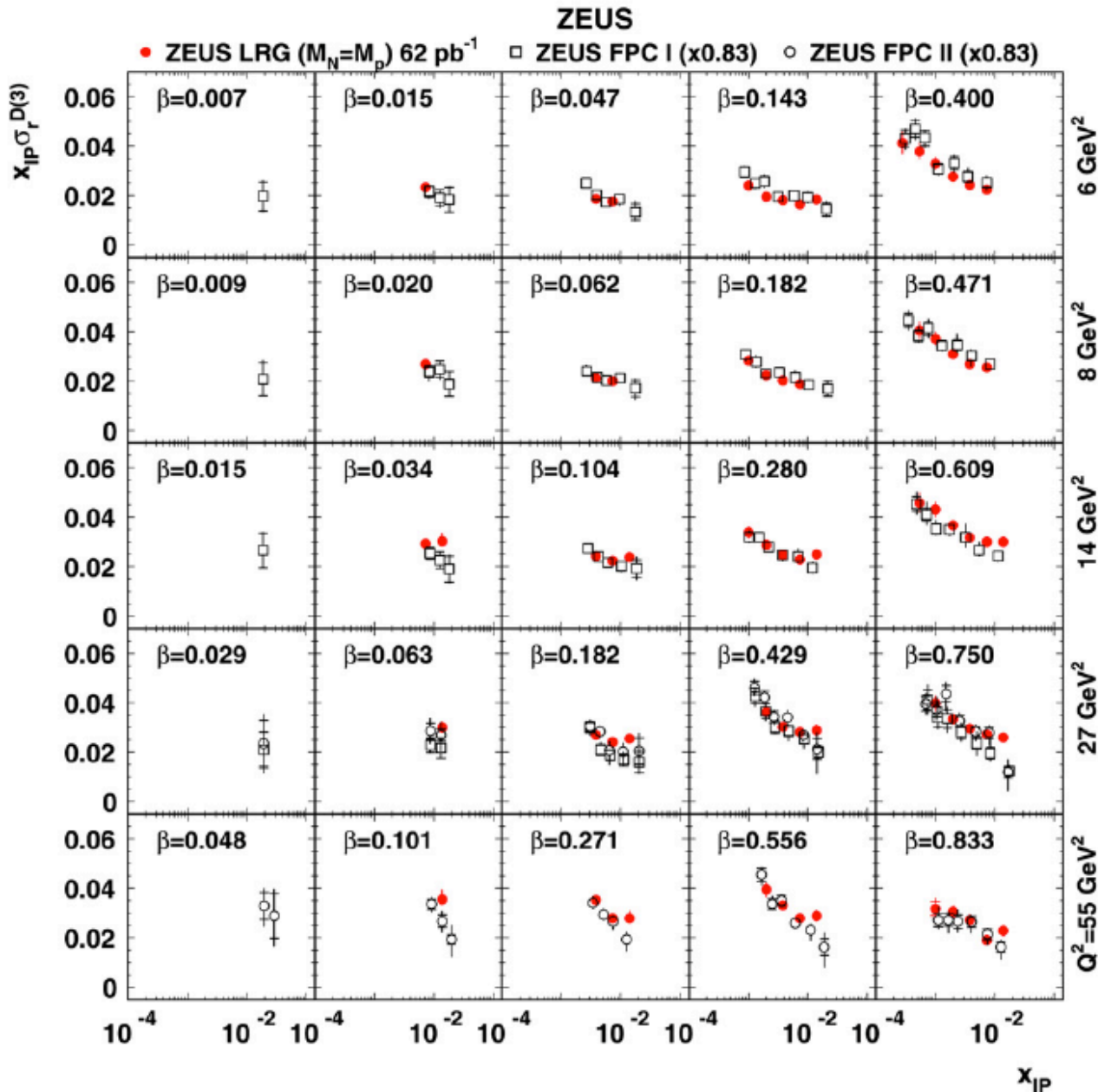
$$\Delta\eta \approx \ln(W^2/M_X^2)$$

ZEUS



M_X and LRG methods have a different sensitivity to the proton dissociation background
some control over p-diss systematic

LRG vs M_X

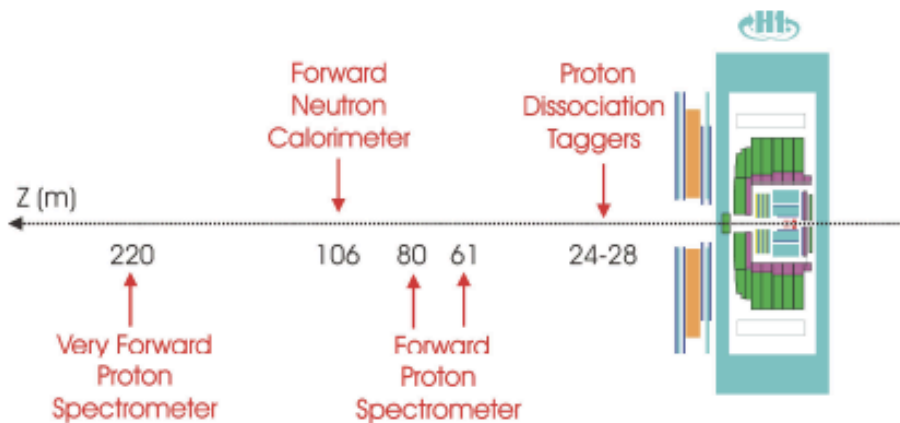


good overall agreement

deviation at large values of x_{IP} are due to different treatment of the reggeon contributions

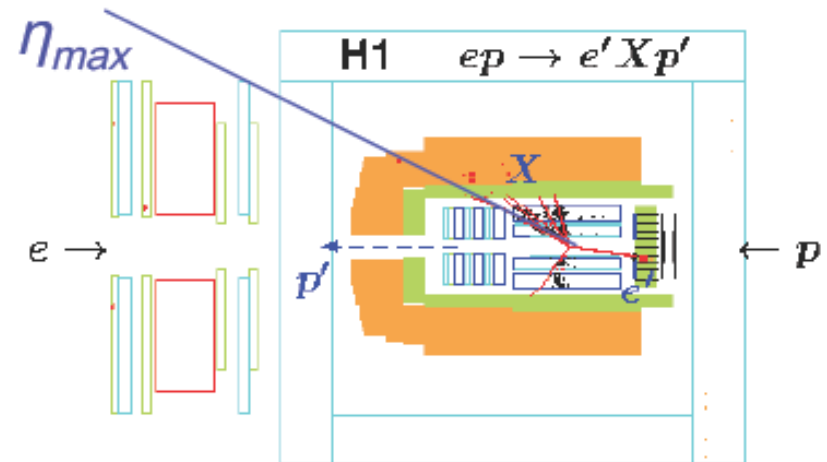
H1 Diffractive Measurements

Scattered proton in Leading Proton Spectrometers (LPS)



Limited by statistics and
p-tagging systematics
(as in ZEUS)

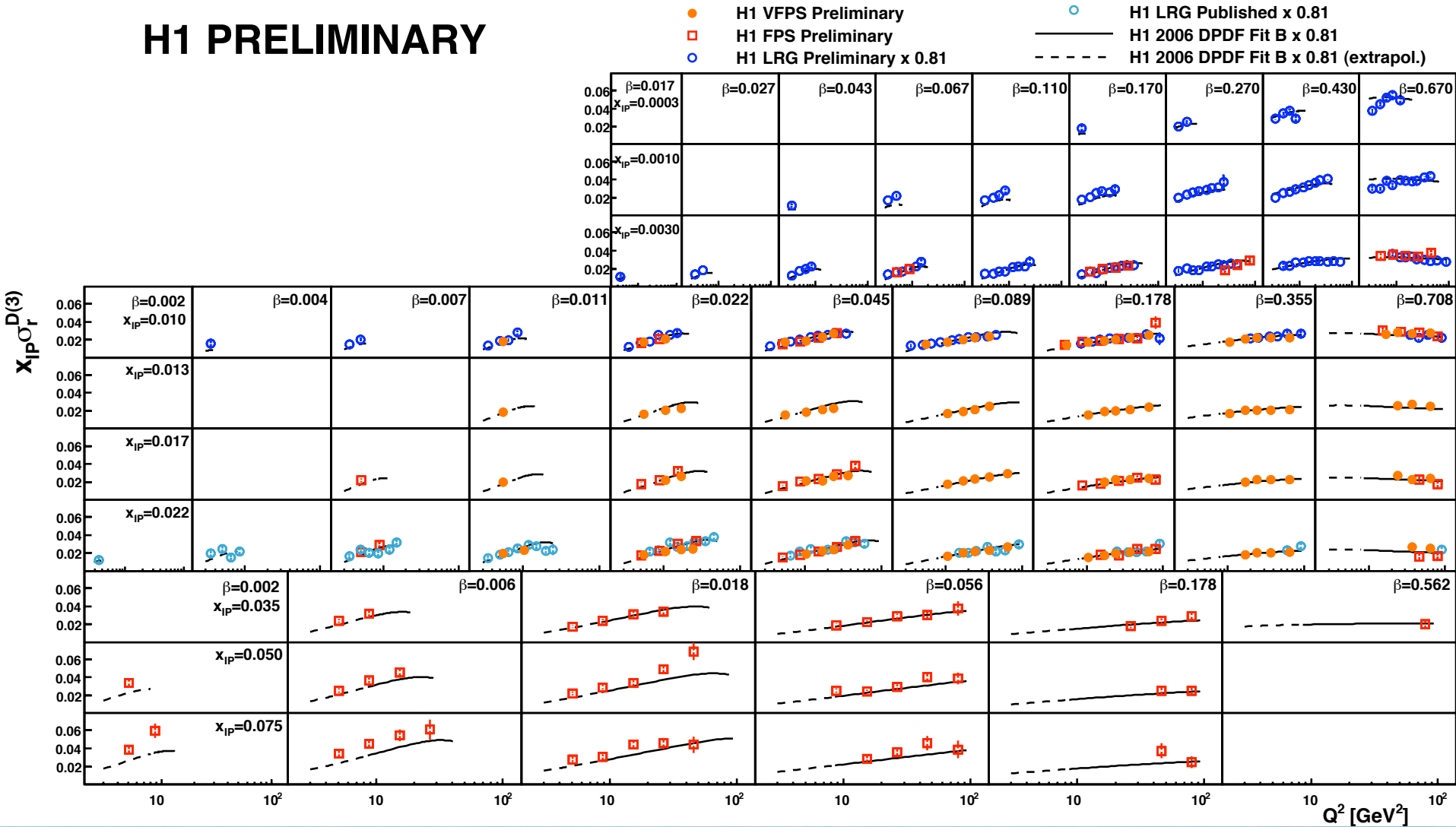
'Large Rapidity Gap' (LRG)
adjacent to outgoing
(untagged) proton



Limited by p-diss systematics
(as in ZEUS)

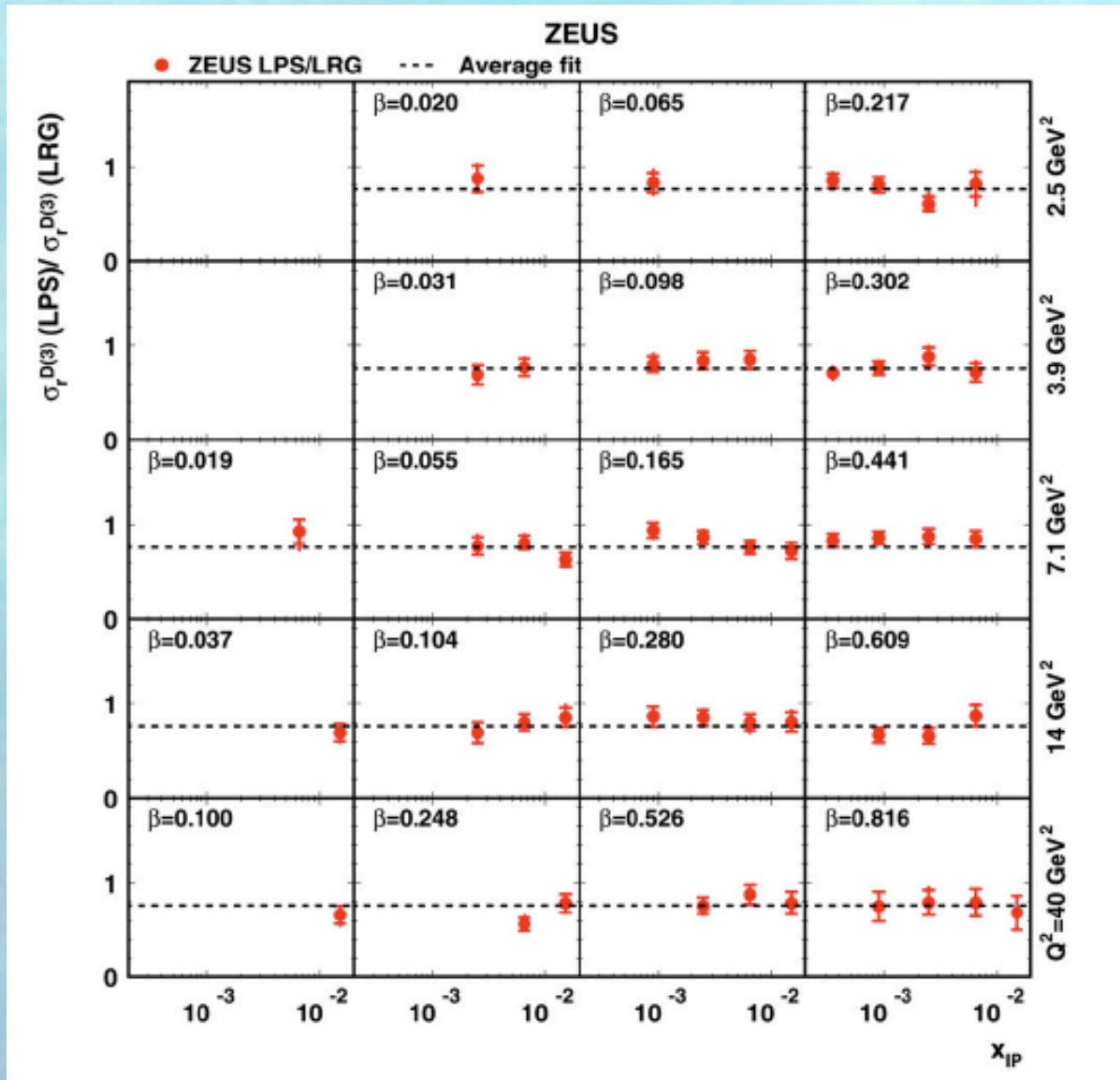
H1 VFPS/FPS/LRG

H1 PRELIMINARY



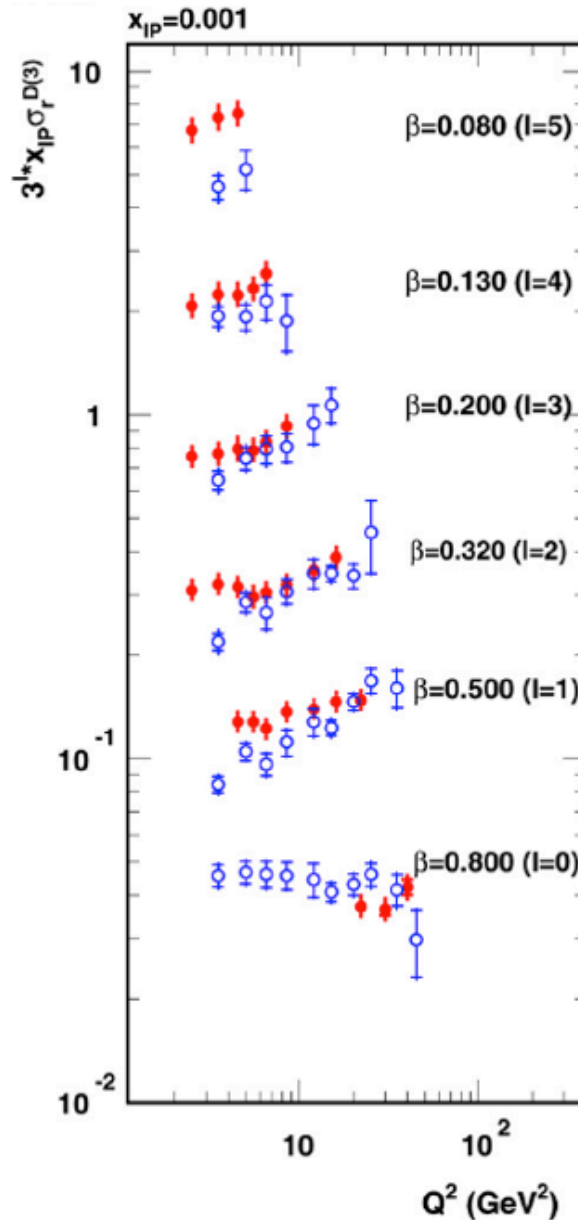
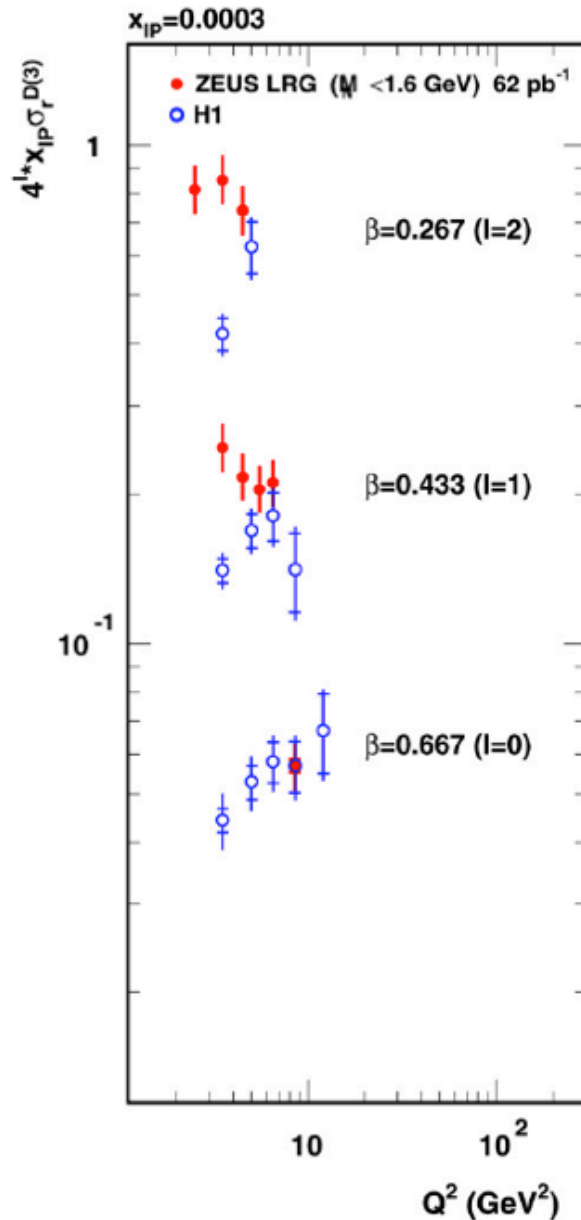
large coverage of phase space and good agreement of the different data sets in regions of mutual coverage

LRG vs LPS



good agreement in shape in regions of mutual coverage
from LPS/LRG \Rightarrow p-diss \sim 20% of LRG for ZEUS and H1

H1-LRG vs ZEUS LRG



comparison of
LRG data is
sensitive to
systematic
effects

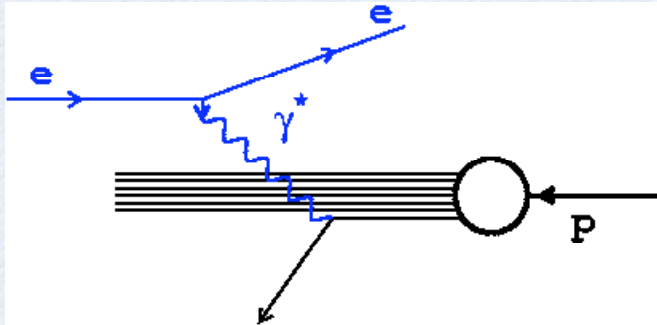
(F_2 data of H1
and ZEUS
agrees very well)

p-diss
systematic
differences?

Much better
agreement
between the
ZEUS and H1
LPS data

Partons vs Dipoles

Infinite momentum frame: Partons



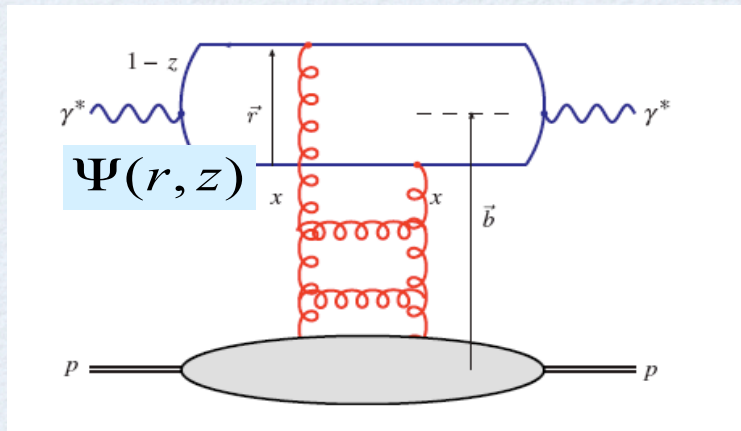
F_2 measures parton density at a scale Q^2

$$F_2 = \sum_f e_f^2 x q(x, Q^2)$$

Proton rest frame: Dipoles - long living quark pair interacts with the gluons of the proton

dipole life time $\approx 1/(m_p x)$

$= 10 - 1000 \text{ fm at } x = 10^{-2} - 10^{-4}$



$$\sigma_{tot}^{\gamma^* p} = \int \Psi^* \sigma_{qq} \Psi ; \quad F_2 = \frac{Q^2}{4\pi^2 \alpha_{em}} \sigma_{tot}^{\gamma^* p}$$

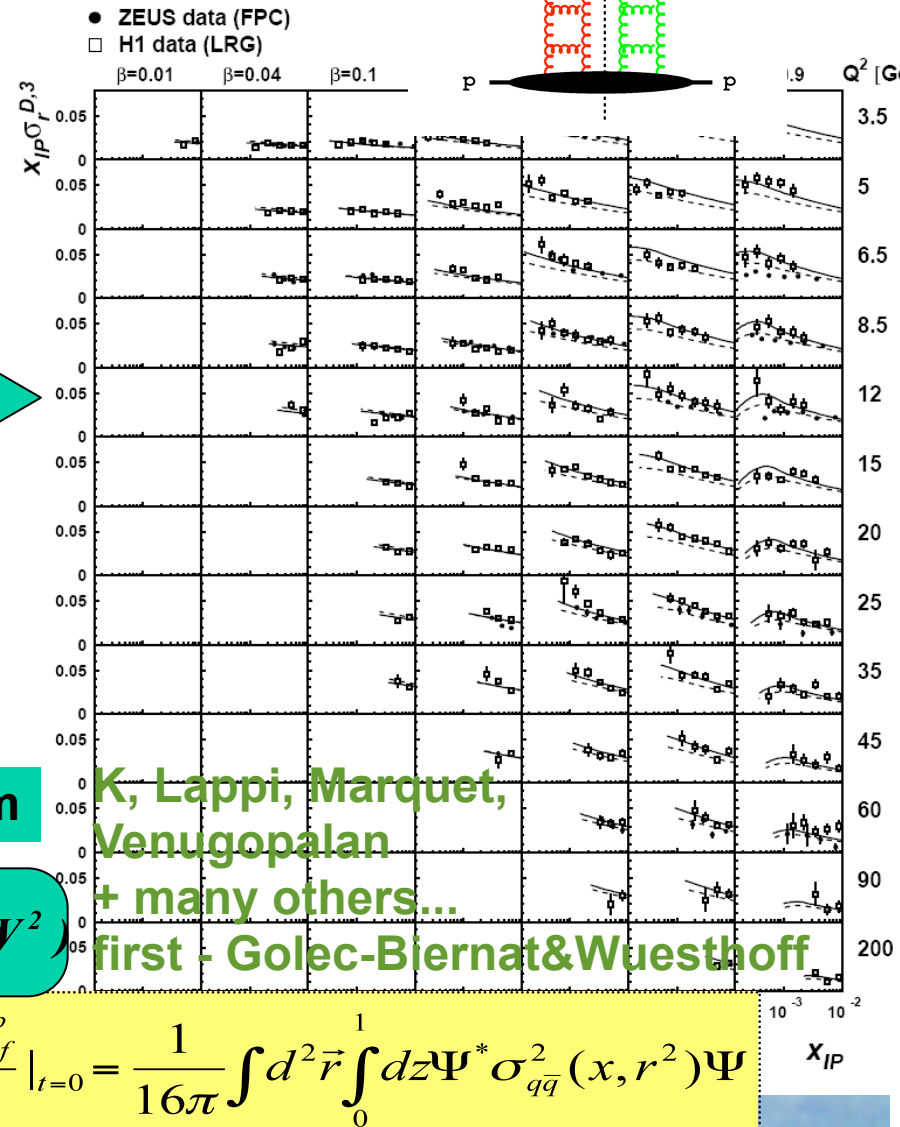
for small dipoles, at low- x , dipole picture is equivalent to the QCD parton picture

$$\sigma_{qq} \sim r^2 x g(x, Q^2)$$

A diagram illustrating the interaction between a proton (p) and a positronium atom (Ps). The proton is represented by a black oval at the bottom, with a horizontal line passing through its center. The positronium atom is represented by a blue oval at the top, with a horizontal line passing through its center. A vertical dashed line connects the centers of the two ovals. A red wavy line, representing a virtual photon, connects the two ovals. The wavy line is labeled with γ^* at both ends, indicating it is a virtual photon. The diagram is labeled 'p' at the bottom and 'Ps' at the top.



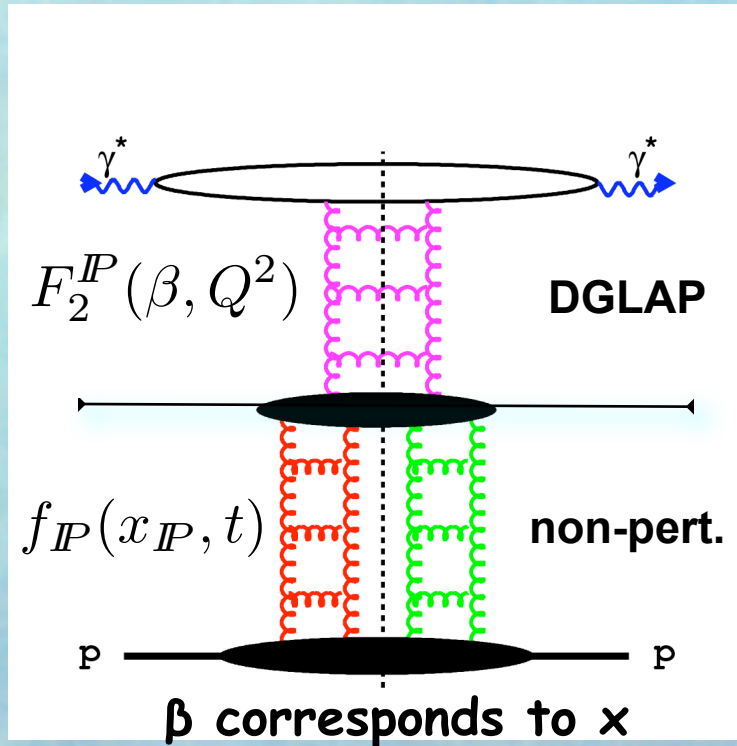
$$\sigma_{tot}^{\gamma^* P} = \frac{1}{W^2} Im A_{el}(W^2)$$



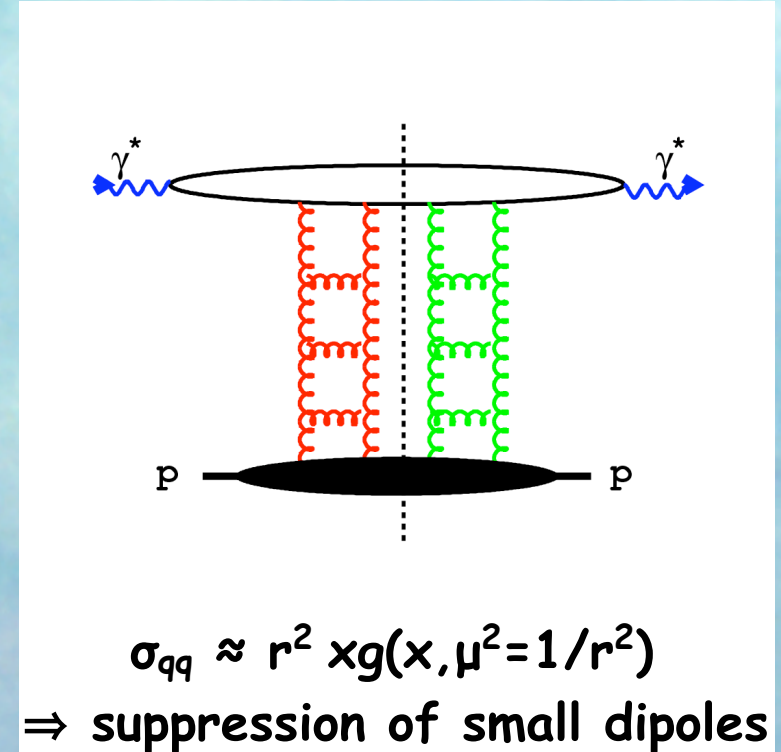
$$\sigma_{tot}^{\gamma^* p} = \int d^2\hat{r} \int_0^1 dz \Psi^* \sigma_{q\bar{q}}(x, r^2) \Psi$$

$$\frac{d\sigma_{diff}^{\gamma^* p}}{dt}\Big|_{t=0} = \frac{1}{16\pi} \int d^2\vec{r} \int_0^1 dz \Psi^* \sigma_{q\bar{q}}^2(x, r^2) \Psi$$

Diffractive structure function approach



Dipole approach



$$F_2^D = f_{\mathbb{P}}(x_{\mathbb{P}}, t) F_2^{\mathbb{P}}(\beta, Q^2)$$

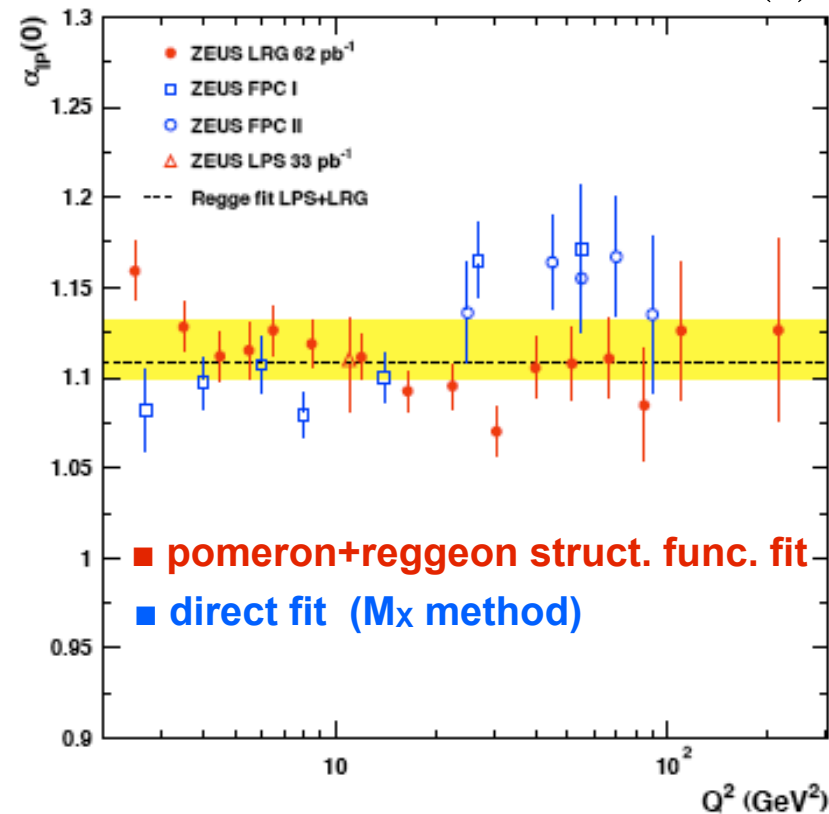
$$f_{\mathbb{P}} = \frac{e^{bt}}{x_{\mathbb{P}}^{2\alpha_{\mathbb{P}} - 1}}$$

$$d\sigma_{diff}^{\gamma^* p}/dt \propto \int dz dr^2 \Psi^* \sigma_{qq}^2(x, r^2, t) \Psi$$

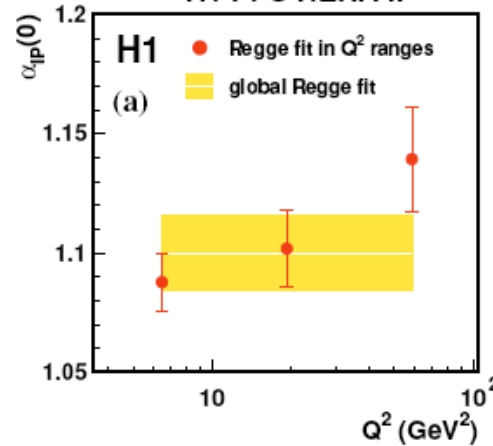
Pomeron intercept

ZEUS

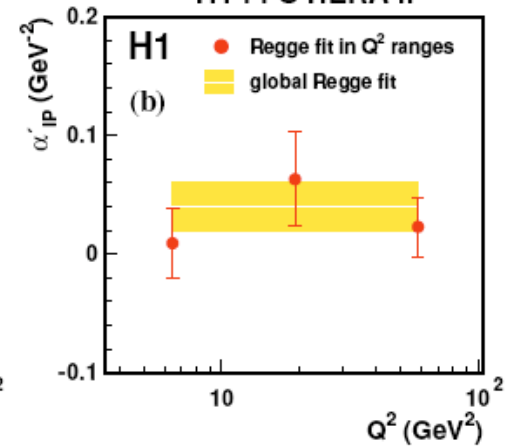
$$\alpha_P(t) = \alpha_P(0) + \alpha' \cdot t$$



H1 FPS HERA II



H1 FPS HERA II



e.g. from H1 FPS - HERA II data:

$$\alpha_P(0) = 1.10 \pm 0.02(\text{exp}) \pm 0.03(\text{model})$$

no strong Q^2 dependence of α_P observed
 in agreement with the dominance of non-perturbative effects in the pomeron SF

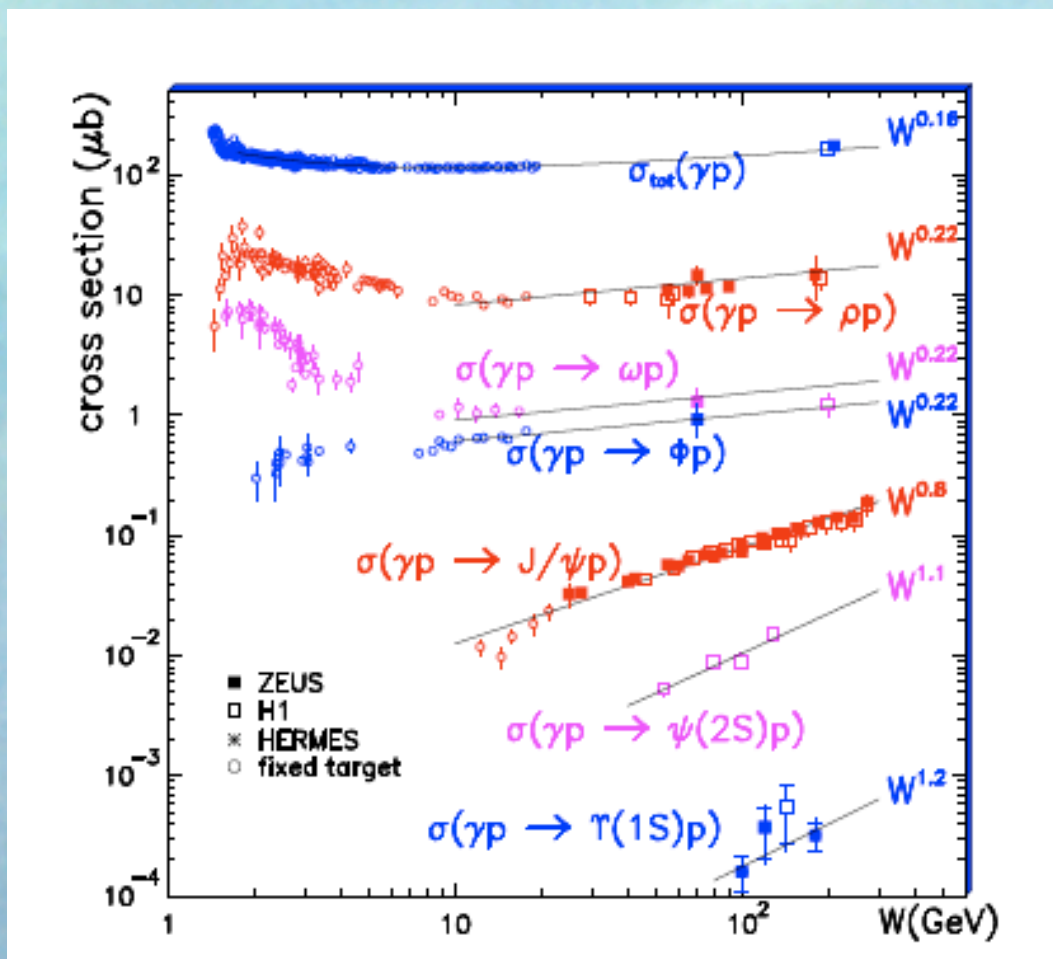
in agreement with the dipole model predictions;
 diffraction selects much larger dipoles than non-diff DIS
 \Rightarrow much weaker Q^2 dependence than in non-diff DIS

Big question for LHC precision measurements:

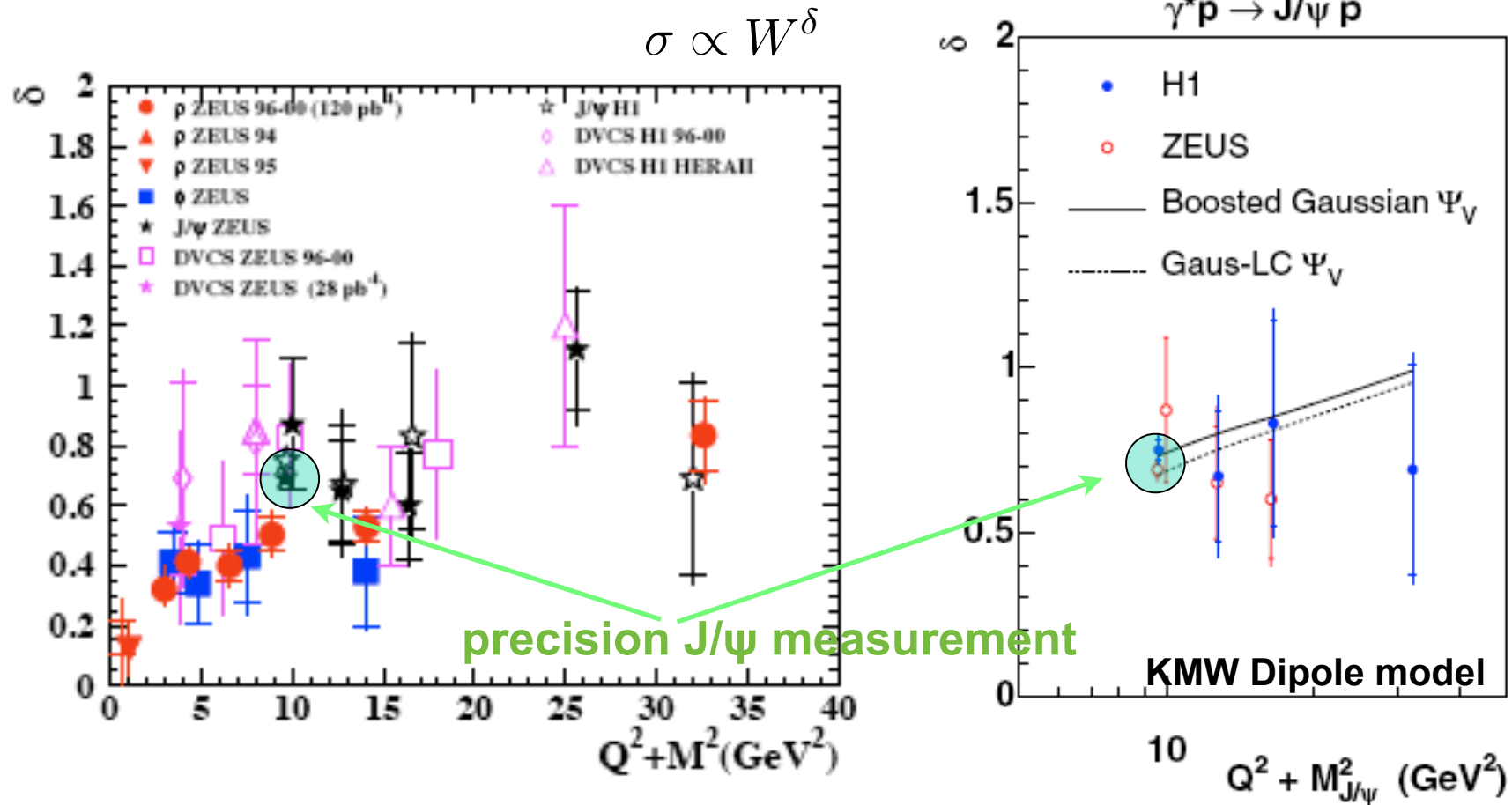
is the inclusive diffractive component evolving with Q^2 like in DGLAP
or like in the dipole model (or even in a more involved way) ?

The inclusive diffractive data do not have enough precision to answer it

Clear hints provided by the exclusive vector meson production

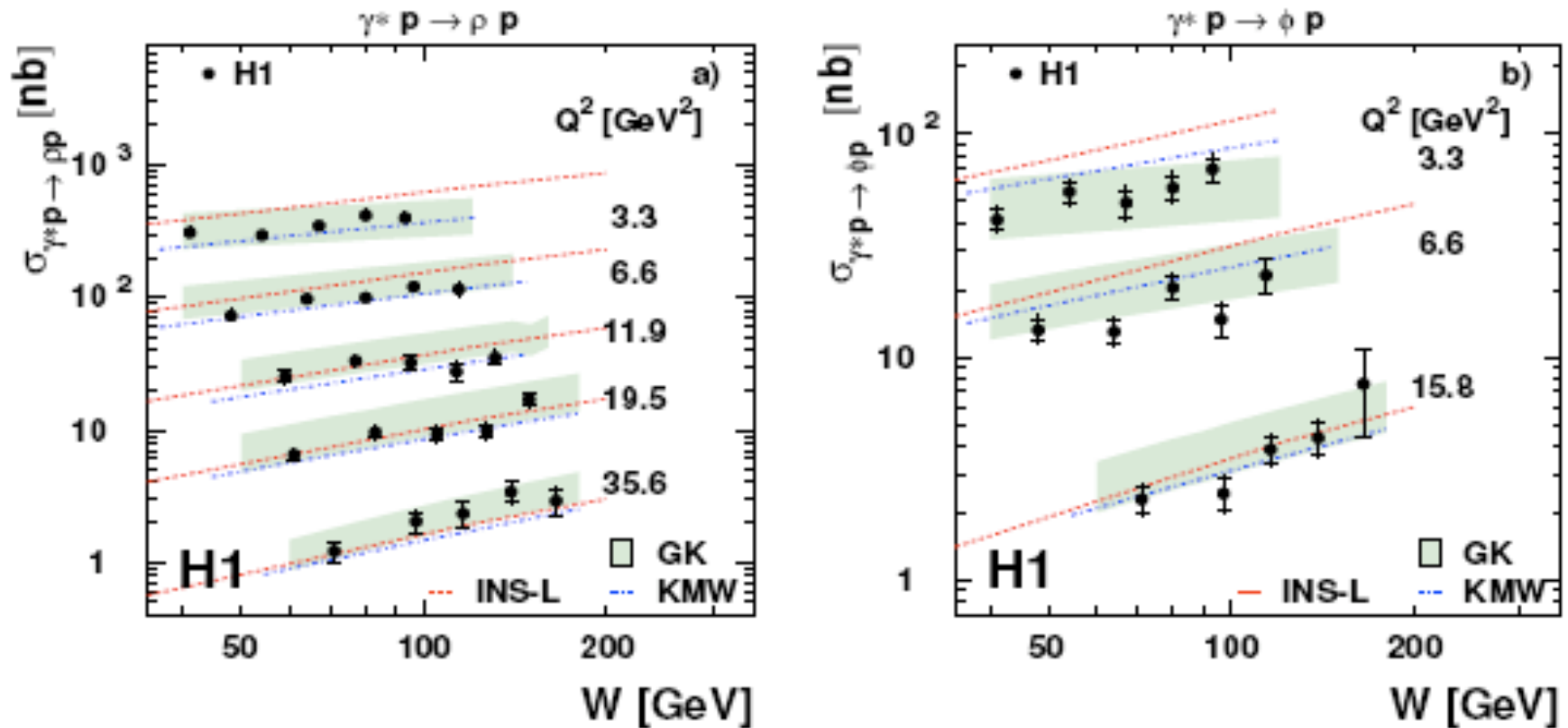


Pomeron intercepts from excl. Vector Mesons



Dipole model with the DGLAP evolution of the gluon density predicts well the δ 's for J/ψ , ρ , ϕ VM and for DVCS

W dependence of exclusive Vector Mesons cross sections

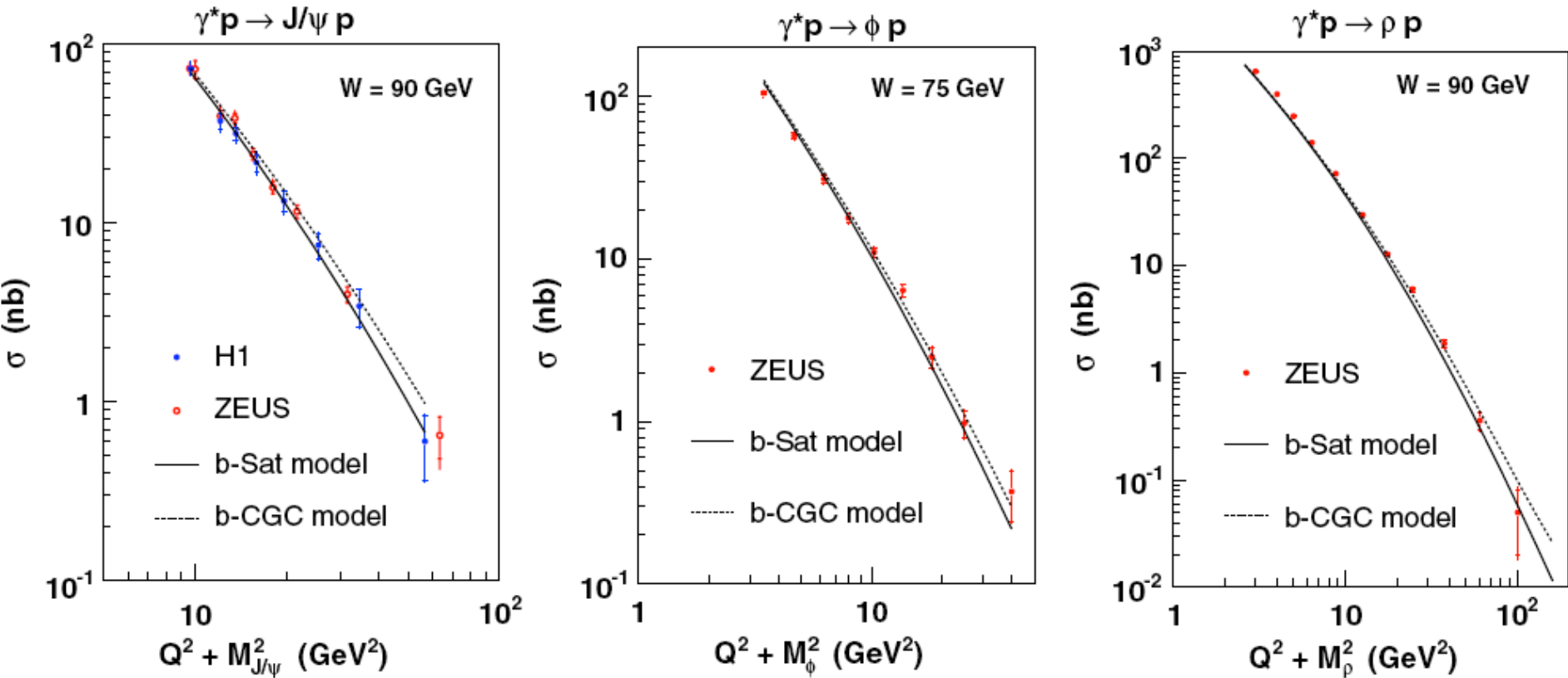


Dipole model with the DGLAP evolution of the gluon density predicts well the rise with W of the ρ and ϕ VM cross sections

Note: these are absolute predictions obtained from the gluon density determined from F_2

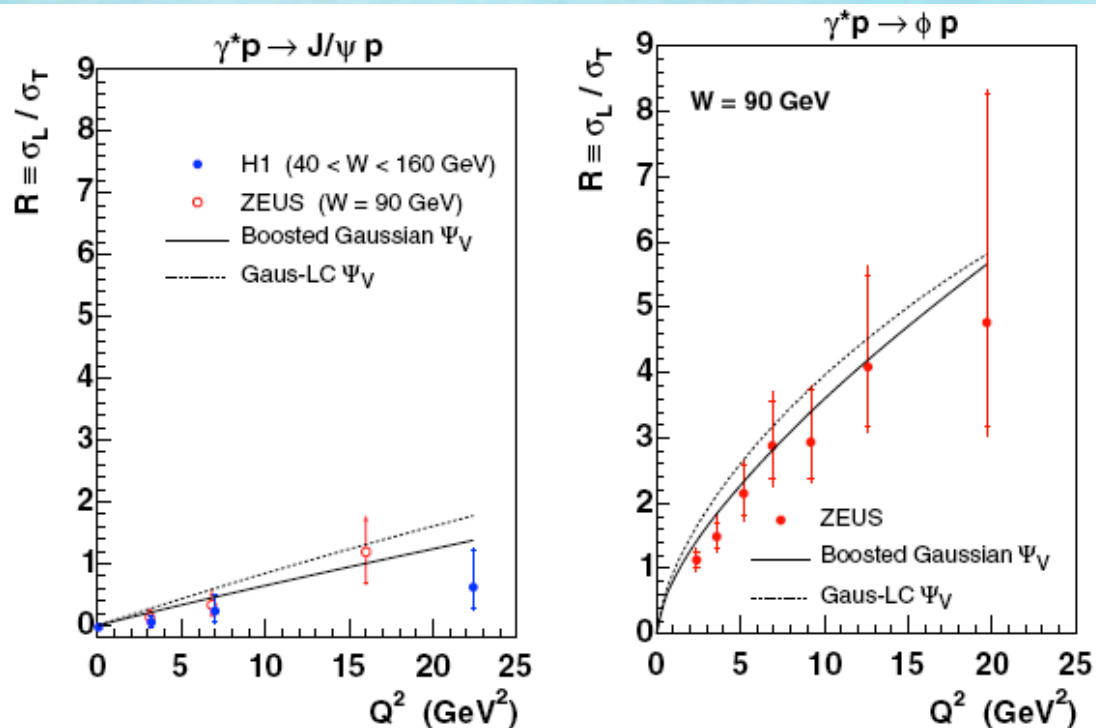
Total VM cross sections from dipole model

KMW Dipole model

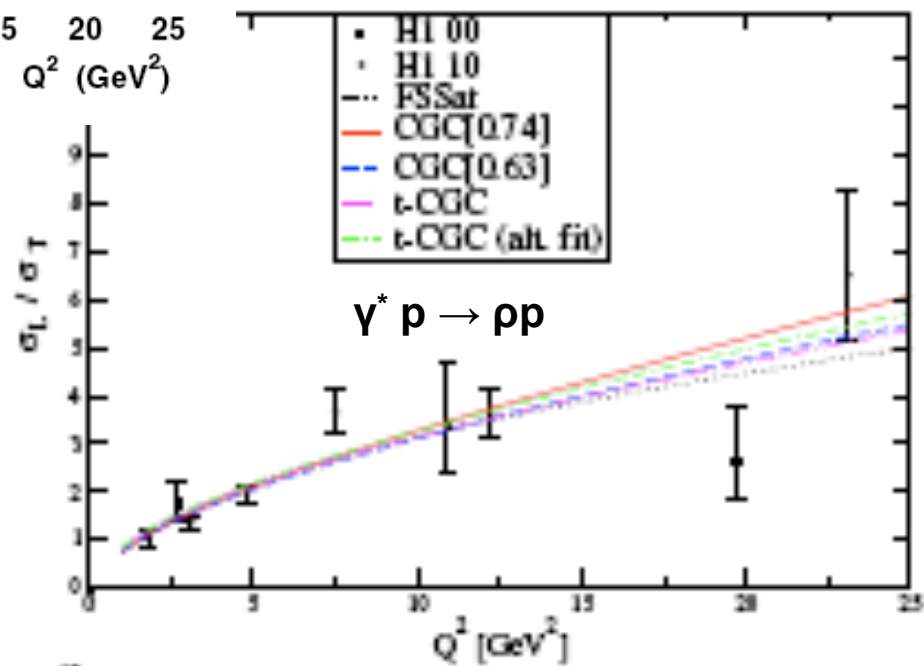


Note: these are absolute predictions obtained from the gluon density determined from F_2

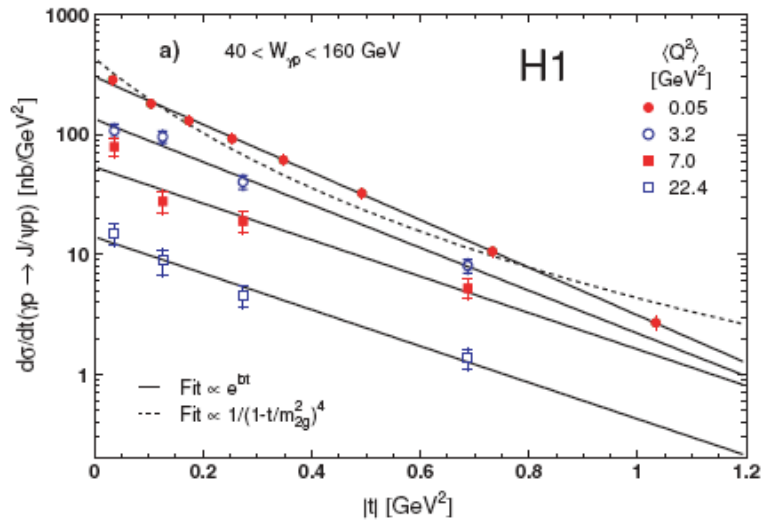
Dipole model description of σ_L / σ_T for VM



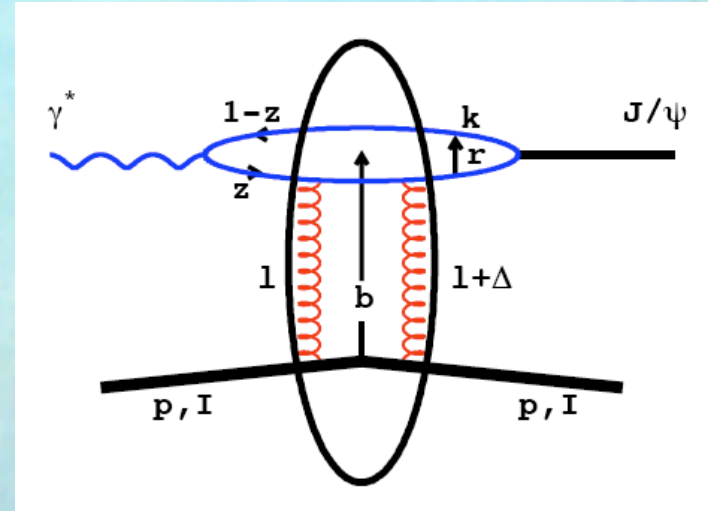
Forshaw and Sandapen improved recently the BG wf by enhancing the end point singularity contributions in the transverse ρ wf



t-distributions



$$\frac{d\sigma}{dt} \sim e^{-b|t|}$$



transverse size of the
interaction region

$$b = b_V + b_p$$

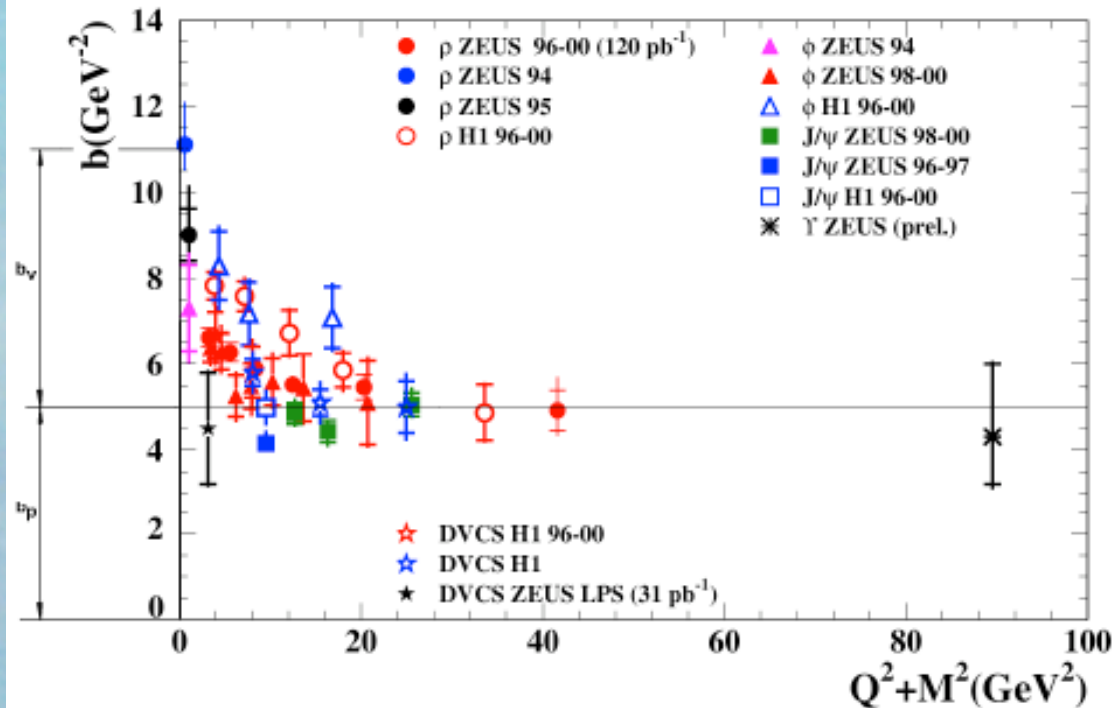
Vector Mesons

$$b_V = 1/(Q^2 + M^2)$$

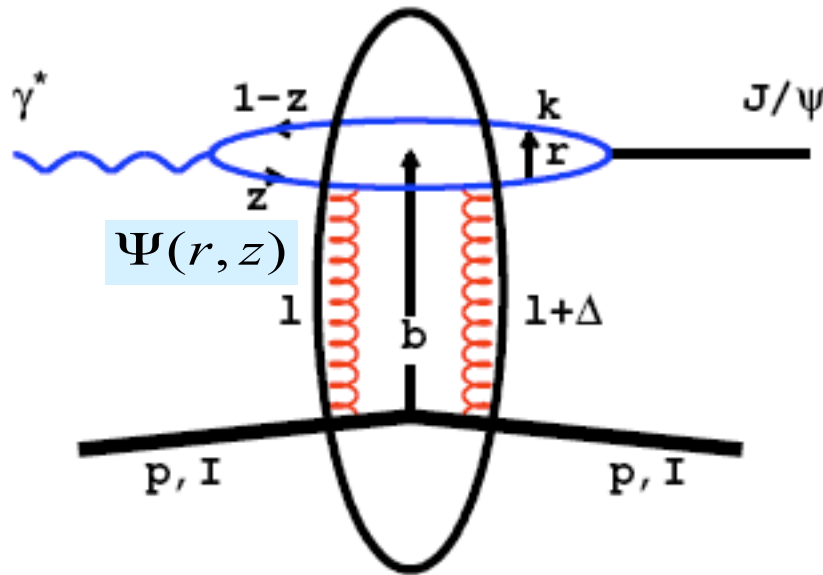
proton

$$b_p \sim 5 \text{ GeV}^2$$

in dip. mod. $b_p \sim 4 \text{ GeV}^2$



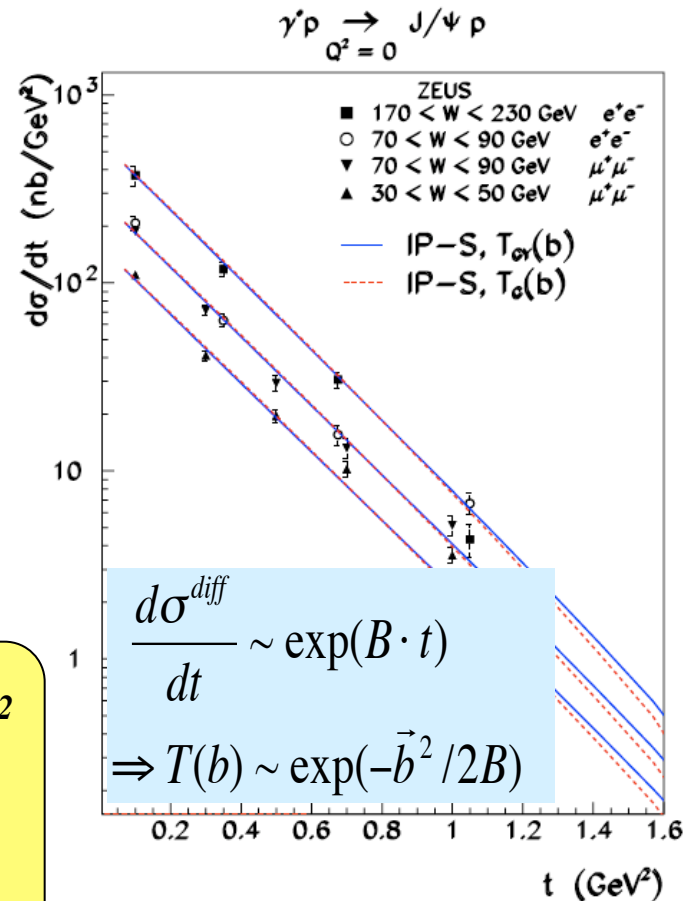
Extracting Proton Shape using dipoles



$$\frac{d\sigma_{VM}^{\gamma^* p}}{dt} = \frac{1}{16\pi} \left| \int e^{-i\vec{b} \cdot \vec{\Delta}} \Psi_{VM}^* 2 \left\{ 1 - \exp\left(-\frac{\Omega}{2}\right) \right\} \Psi \right|^2$$

$$\Omega = \frac{\pi^2}{N_C} r^2 \alpha_s(\mu^2) x g(x, \mu^2) T(b)$$

T(b)-proton shape

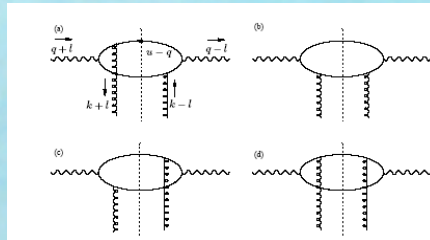


KT, KMW

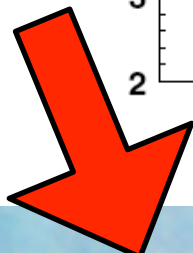
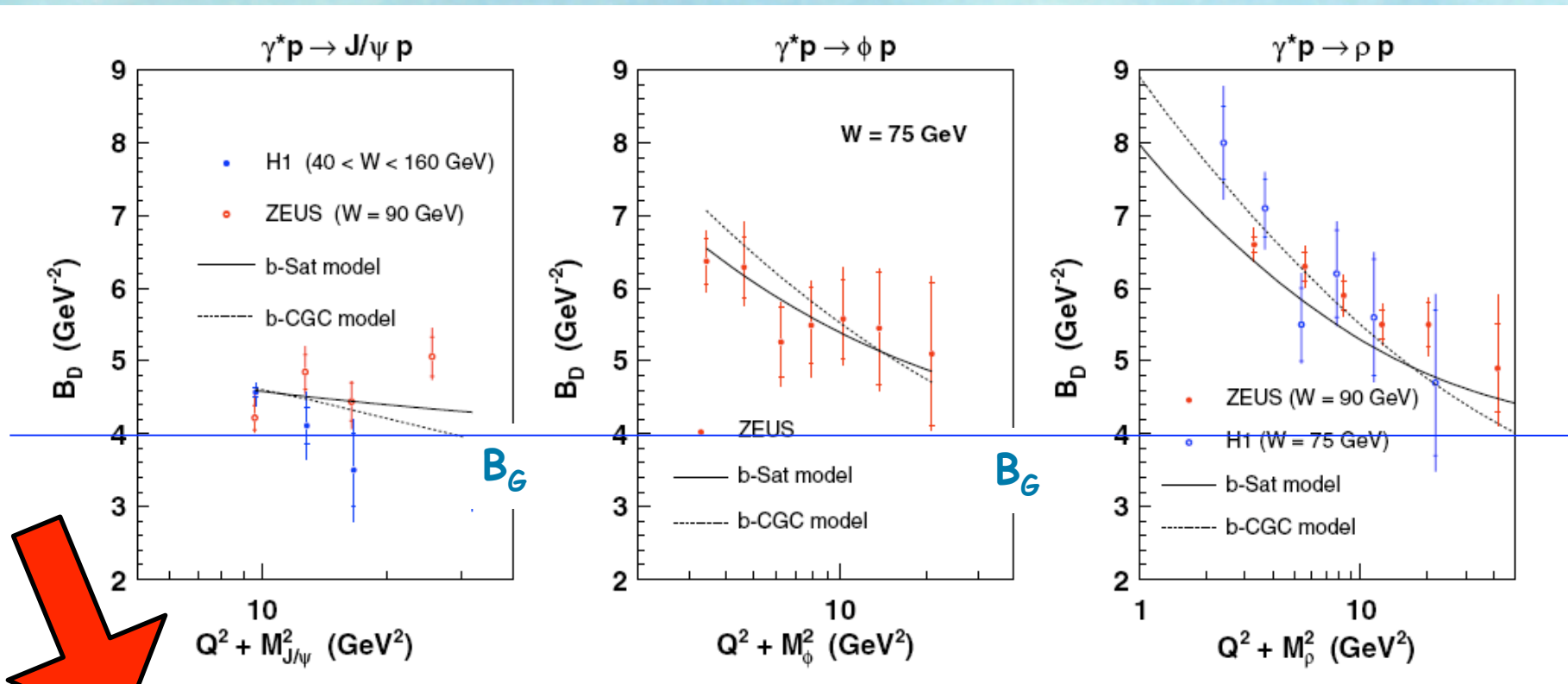
The size of interaction region B for various VM

Modification by Bartels,
Golec-Biernat, Peters

$$e^{i\vec{b} \cdot \vec{\Delta}} \Rightarrow e^{i(\vec{b} + (1-z)\vec{r}) \cdot \vec{\Delta}}$$



KMW



2g proton radius

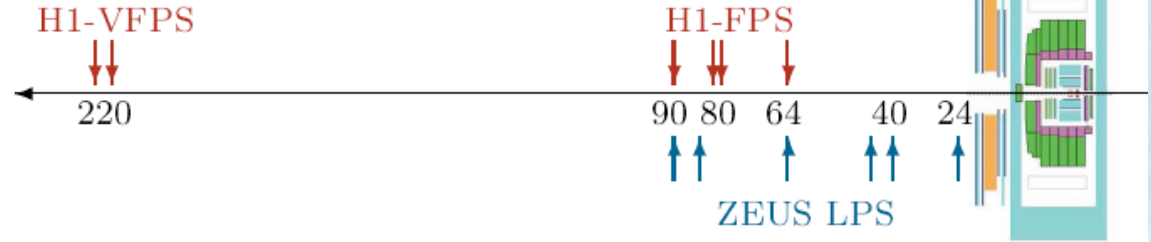
$$\sqrt{\langle r_{2g}^2 \rangle} = \sqrt{3 \cdot B_G} = 0.61 \pm 0.04 \text{ fm.}$$

charged

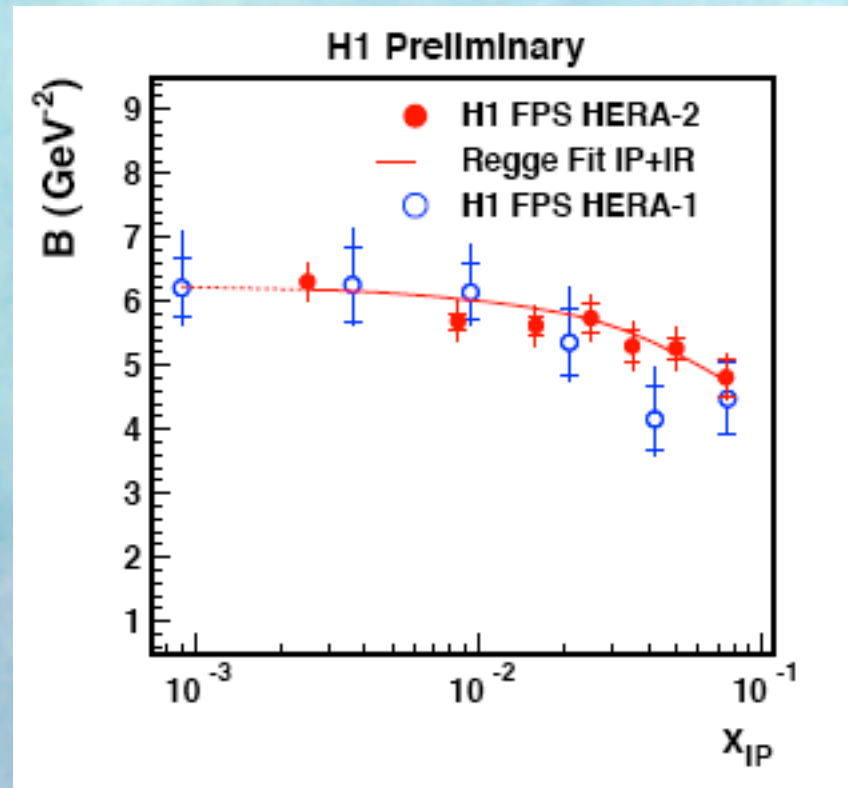
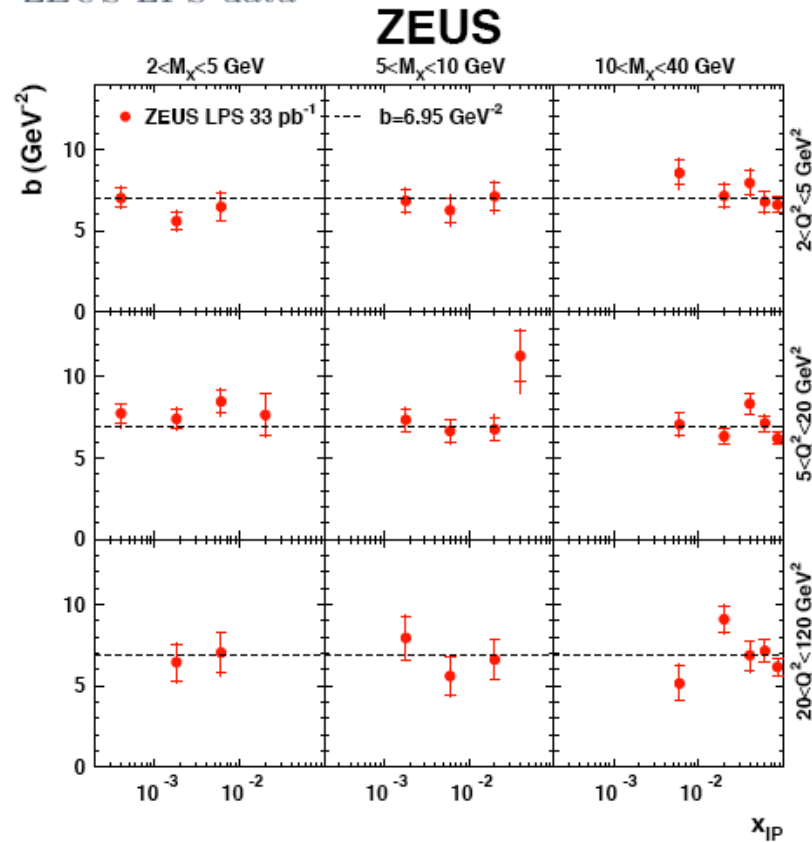
$$r_p = 0.875 \pm 0.007 \text{ fm.}$$

B in inclusive diffraction

Roman Pot Method

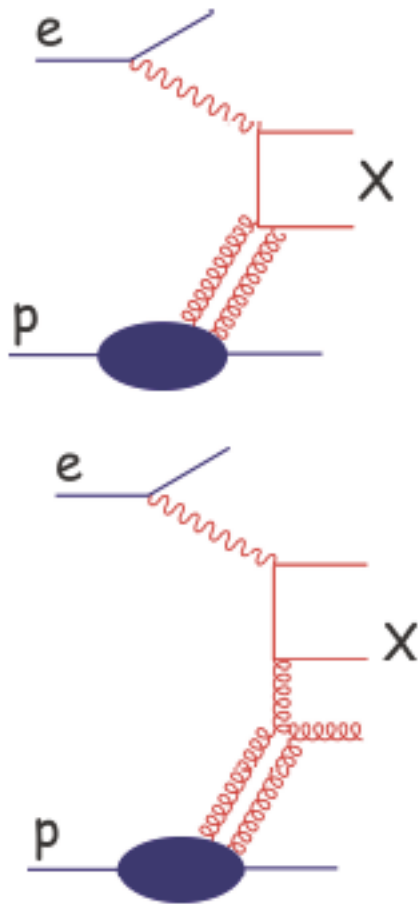


ZEUS-LPS data

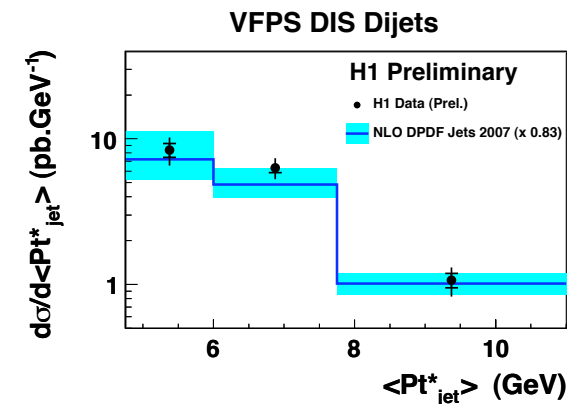
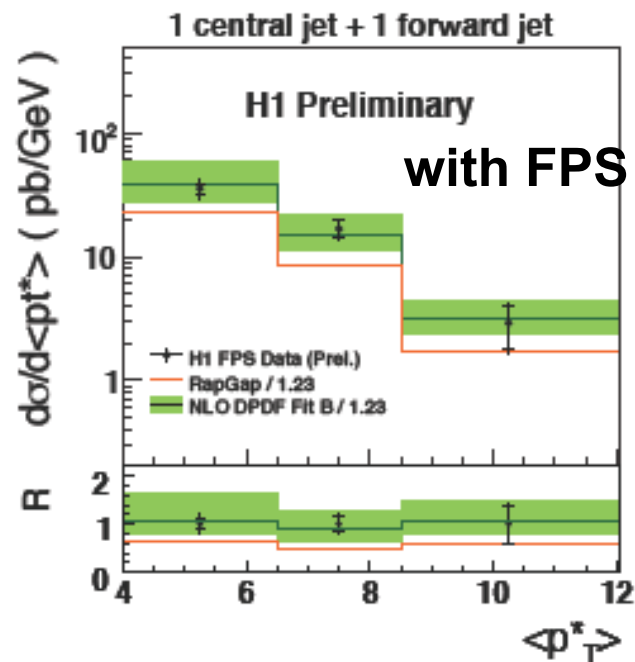
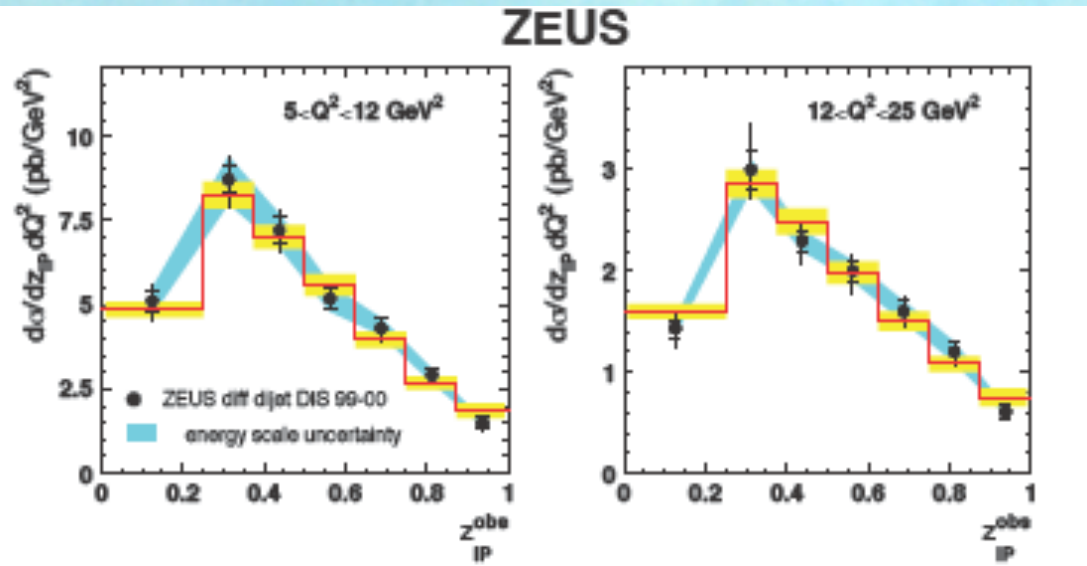


no dependence of B from Q^2 observed
 in agreement with the expected dominance of large dipoles?
 precise evaluation in dipole model is still missing

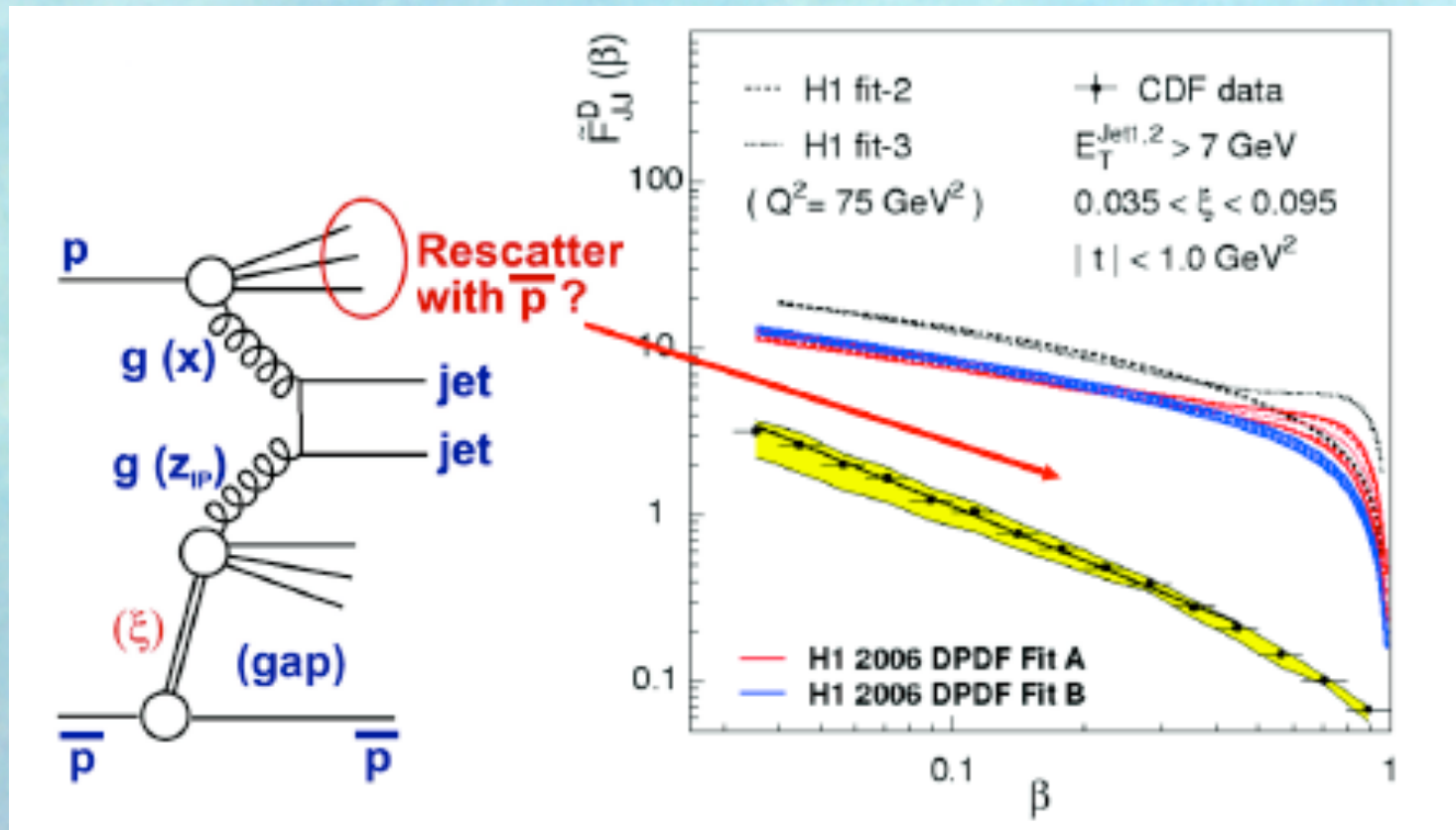
Diffractive jets



good description of diffractive jets with diffractive structure functions, DPDFs



Diffractive jets at pp



Evidence for strong absorptive effects in comparing diffractive jets in pp with HERA DPDFs predictions

$S^2 \sim 0.1$ at Tevatron,
 S^2 is expected to be significantly smaller at LHC

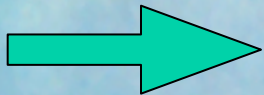
Conclusions

Diffraction is a substantial part of DIS reaction

The success of the dipole description of the vector meson production (based on the gluon density determined in F_2) strongly indicates the existence of an universal hard Pomeron.

Inclusive diffractive data show that this pomeron is also soft, in agreement with the properties of a QCD-BFKL Pomeron which is hard and soft simultaneously

Good agreement of inclusive diffractive jet predictions based on DPDF's together with Tevatron data



**strong absorption of hard diffractive processes at LHC
e.g: diffractive Higgs, abundance of MI**

**Properties of the
Discrete Pomeron Solution
(DPS)
of the BFKL equation**

a determination from HERA data

**H. Kowalski, L.N. Lipatov, D.A. Ross
with a collaboration of
J. Ellis, G. Watt**

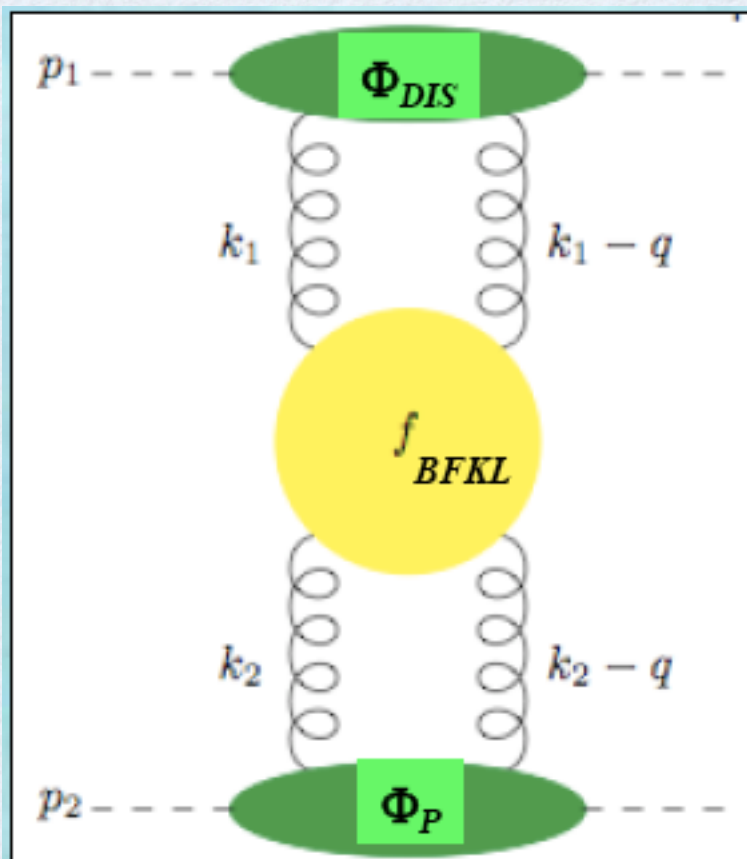
[arXiv:1109.0432v1](https://arxiv.org/abs/1109.0432v1)

Eur. Phys. J. C (2010) 70: 983–998

Physics Letters B 668 (2008) 51–56

The dynamics of Gluon Density at low x is determined by the amplitude for the scattering of a gluon on a gluon, described by the BFKL equation

$$\frac{\partial}{\partial \ln s} \mathcal{A}(s, \mathbf{k}, \mathbf{k}') = \delta(k^2 - k'^2) + \int dq^2 \mathcal{K}(\mathbf{k}, \mathbf{q}) \mathcal{A}(s, \mathbf{q}, \mathbf{k}')$$



which can be solved in terms of the eigenfunctions of the kernel

$$\int dk'^2 \mathcal{K}(\mathbf{k}, \mathbf{k}') f_\omega(\mathbf{k}') = \omega f_\omega(\mathbf{k})$$

in LO, with
fixed α_s

$$f_\omega(\mathbf{k}) = (k^2)^{i\nu-1/2}$$

$$\omega = \alpha_s \chi_0(\nu)$$

prevailing intuition (based on DGLAP) -
gluon are a gas of particles
BFKL leads to a richer structure -
basic feature: oscillations

Properties of the BFKL Kernel

Quasi-locality

$$\mathcal{K}(\mathbf{k}, \mathbf{k}') = \frac{1}{kk'} \sum_{n=0}^{\infty} c_n \delta^{(n)}(\ln(\mathbf{k}^2 / \mathbf{k}'^2))$$

$$c_n = \int_0^{\infty} dk'{}^2 \mathcal{K}(\mathbf{k}, \mathbf{k}') \frac{k}{k'} \frac{1}{n!} (\ln(\mathbf{k}^2 / \mathbf{k}'^2))^n$$

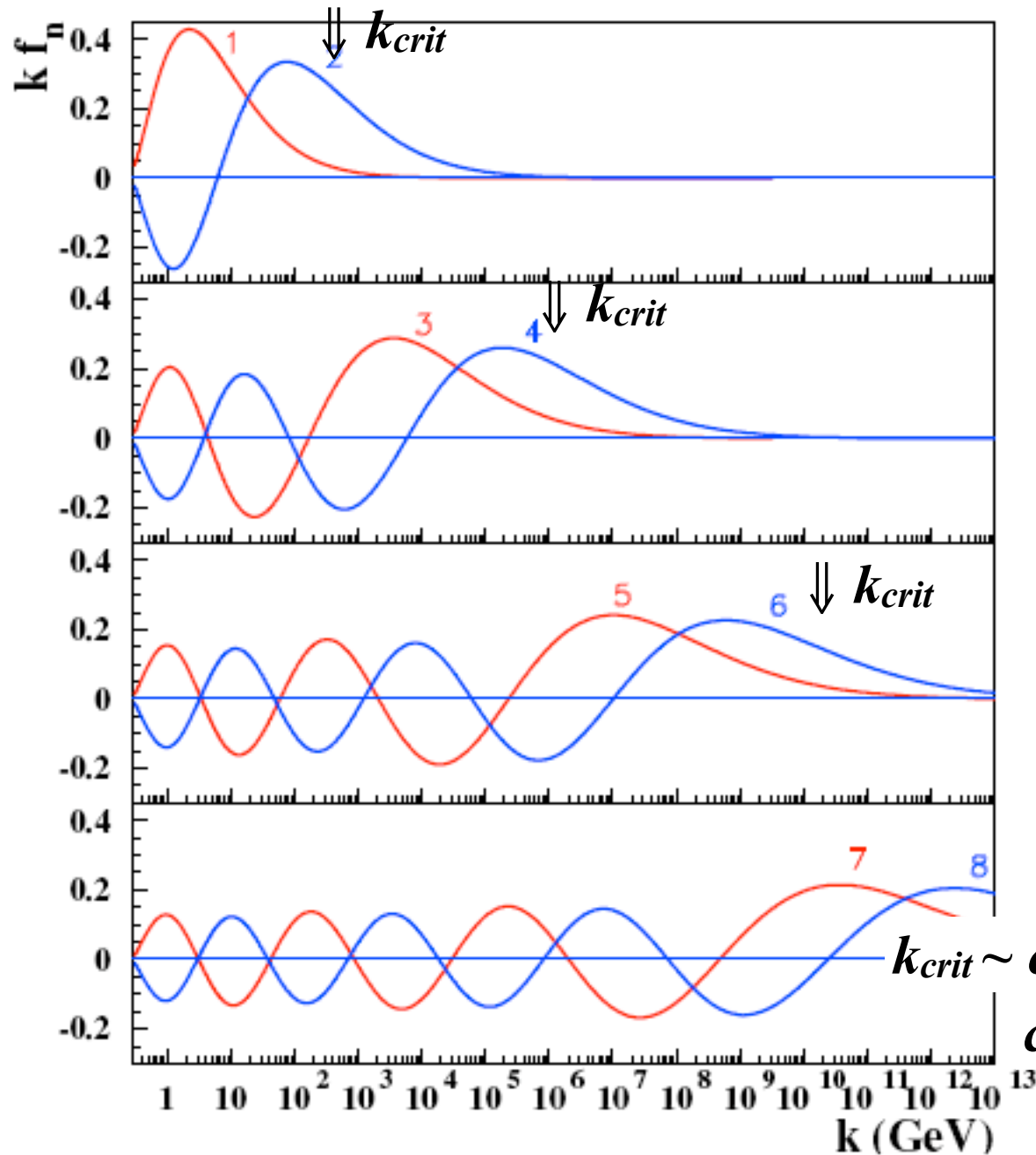
Similarity to the Schroedinger equation

$$k \int dk'{}^2 \mathcal{K}(\mathbf{k}, \mathbf{k}') f_{\omega}(\mathbf{k}') = \sum_{n=0}^{\infty} c_n \left(\frac{d}{d \ln(\mathbf{k}^2)} \right)^n \bar{f}_{\omega}(\mathbf{k}) = \omega \bar{f}_{\omega}(\mathbf{k})$$

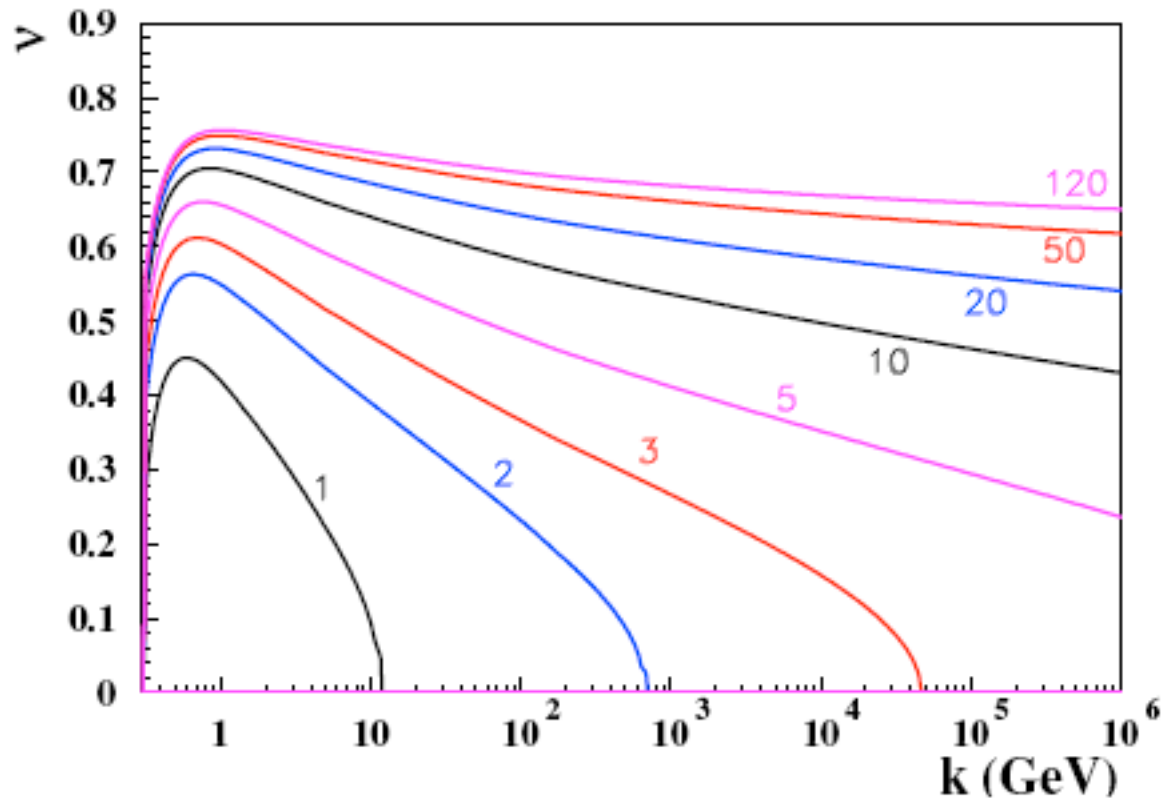
Characteristic function

$$k \int dk'{}^2 \mathcal{K}(\mathbf{k}, \mathbf{k}') f_{\omega}(\mathbf{k}') = \chi \left(-i \frac{d}{d \ln k^2}, \alpha_s(k^2) \right) \bar{f}_{\omega}(k) = \omega \bar{f}_{\omega}(k)$$

The first
eight
eigenfunctions
determined at
 $\eta=0$

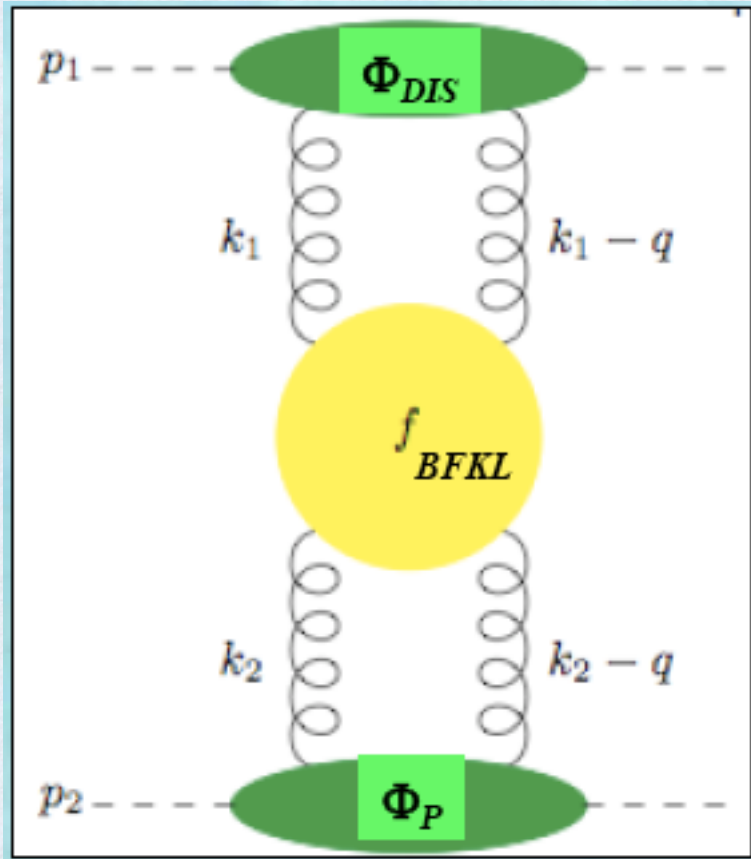


The frequencies $\nu(k)$



Music analogy:
eigenfunctions are tones with modulated
frequencies

Comparison with HERA data



Discreet Pomeron Green function

$$A(\mathbf{k}, \mathbf{k}') = \sum_{m,n} f_m(\mathbf{k}) \mathcal{N}_{mn}^{-1} f_n(\mathbf{k}') \left(\frac{s}{kk'} \right)^{\omega_n}.$$

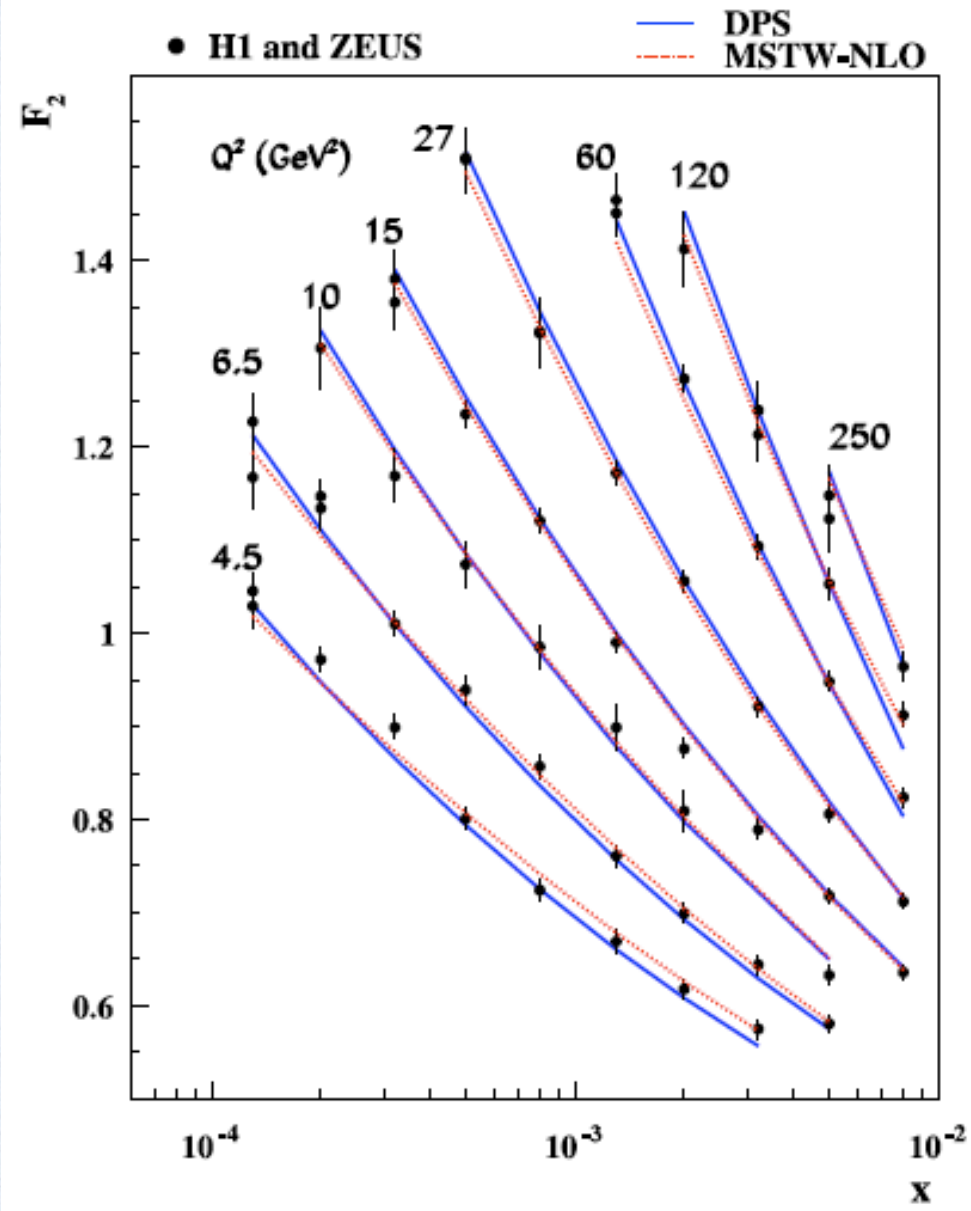
**Integrate with the photon and
proton impact factors**

$$\mathcal{A}_n^{(U)} \equiv \int_x^1 \frac{d\xi}{\xi} \int \frac{dk}{k} \Phi_{DIS}(Q^2, k, \xi) \left(\frac{\xi k}{x} \right)^{\omega_n} f_n(\mathbf{k})$$

$$\mathcal{A}_m^{(D)} \equiv \int \frac{dk'}{k'} \Phi_p(k') \left(\frac{1}{k'} \right)^{\omega_m} f_m(\mathbf{k}').$$

$$F_2(x, Q^2) = \sum_{m,n} \mathcal{A}_n^{(U)} \mathcal{N}_{nm}^{-1} \mathcal{A}_m^{(D)}$$

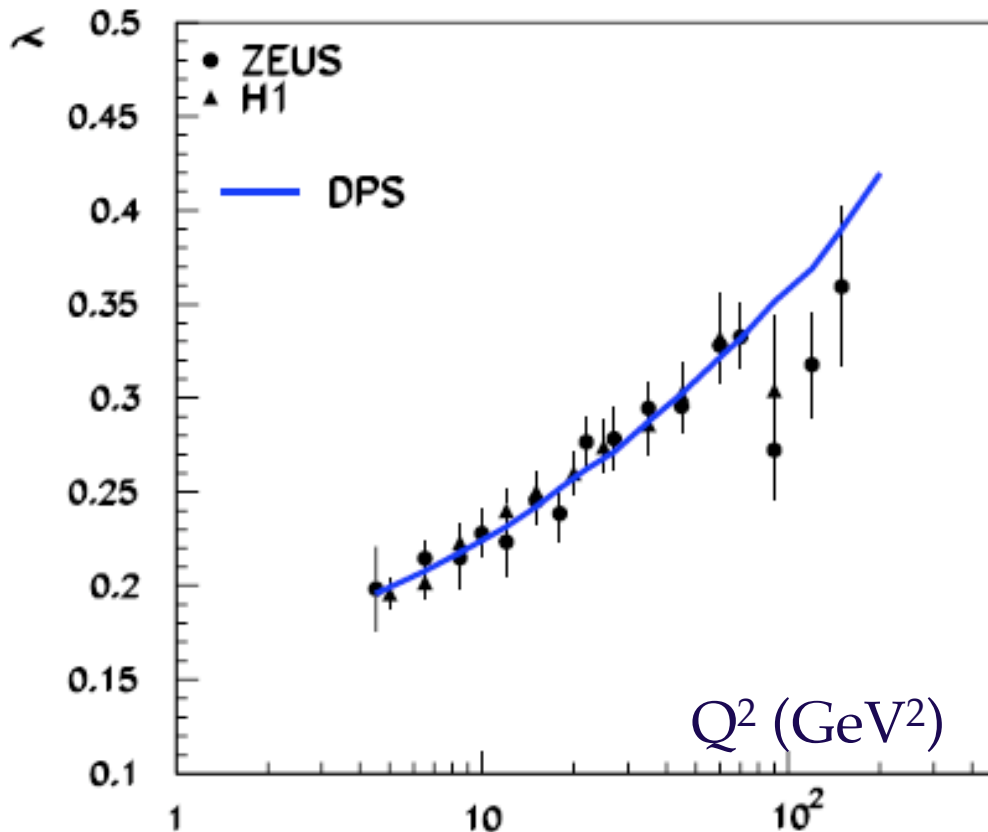
The final fit
performed
with 120 ef's
and 30
overlaps and
5 flavours



χ^2/N_{df}	κ	A	b
154.7 / 125	0.65	1660	20.6

The rate of rise λ

$$F_2 \sim (1/x)^\lambda$$



The first successful pure BFKL description of the λ plot.

For many years it was claimed that BFKL analysis was not applicable to HERA data because of the observed substantial variation of λ with Q^2

DPS frequencies

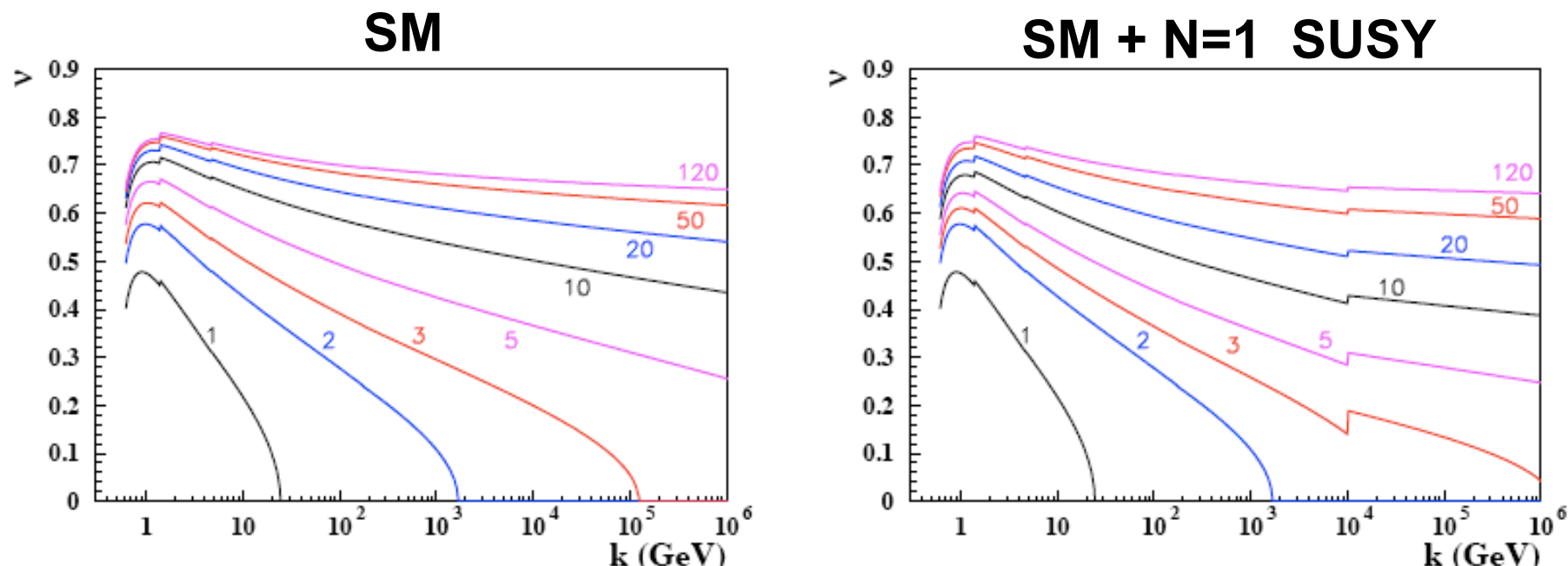
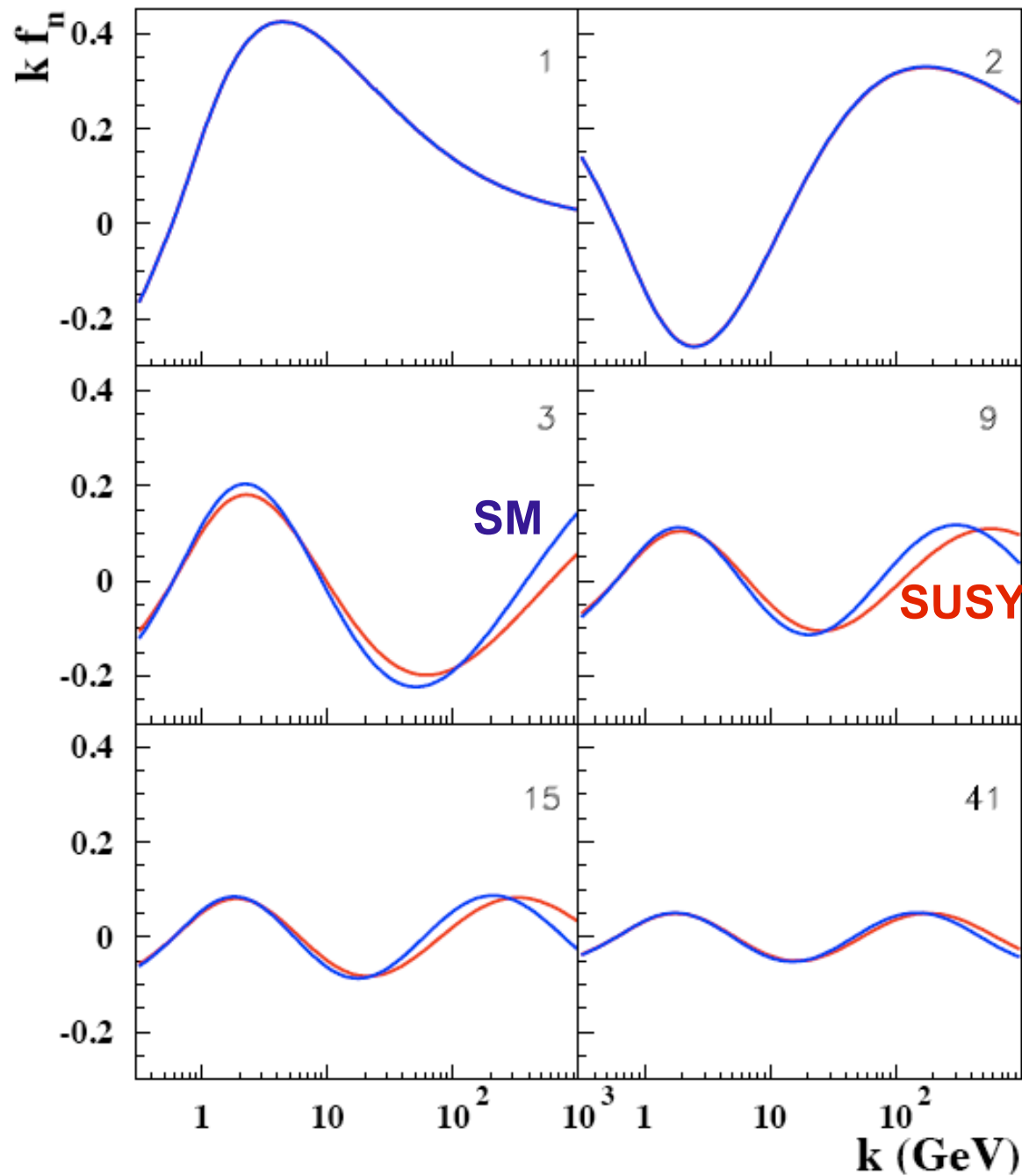


Figure 2: Oscillation frequencies as a function of gluon transverse momentum for various eigenfunctions. The left-hand pane is the case of the Standard Model and the right-hand pane is the case of N=1 SUSY above a threshold of 10 TeV. For the purpose of this comparison it has been assumed that the infrared phases are the same in both cases.

DSP eigenfunction



Backup slides

SUSY Scale (TeV)	χ^2	κ	\tilde{k}_0 (GeV)	η_0	A	b
3	125.7	0.555	0.288	-0.87	201.2	10.6
6	114.1	0.575	0.279	-0.880	464.8	15.0
10	109.9	0.565	0.275	-0.860	720.1	17.7
15	110.1	0.555	0.279	-0.860	882.2	18.6
30	117.8	0.582	0.278	-0.870	561.6	16.2
50	114.9	0.580	0.279	-0.870	627.4	16.8
90	114.8	0.580	0.279	-0.870	700.2	17.5
∞	122.5	0.600	0.274	-0.800	813.1	17.5

Table 1: Fits for N=1 SUSY at different scales. The bottom row corresponds to the Standard Model. All fits are performed with $n_{max} = 100$.

Indirect Evidence for New Physics at the 10 TeV Scale

H. Kowalski ¹, L.N. Lipatov ², and D.A. Ross ³

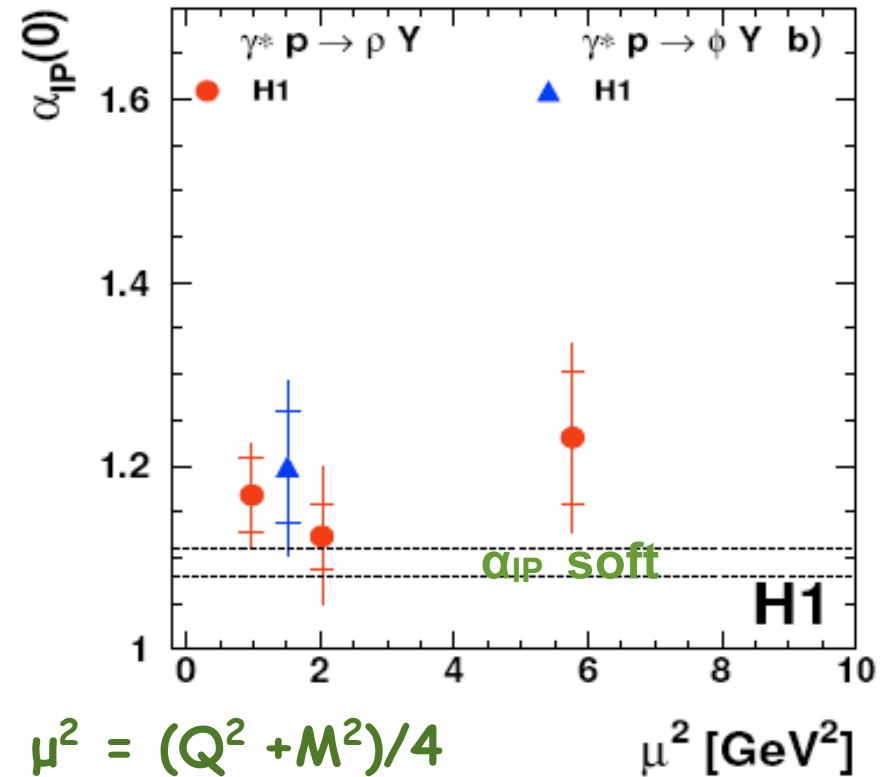
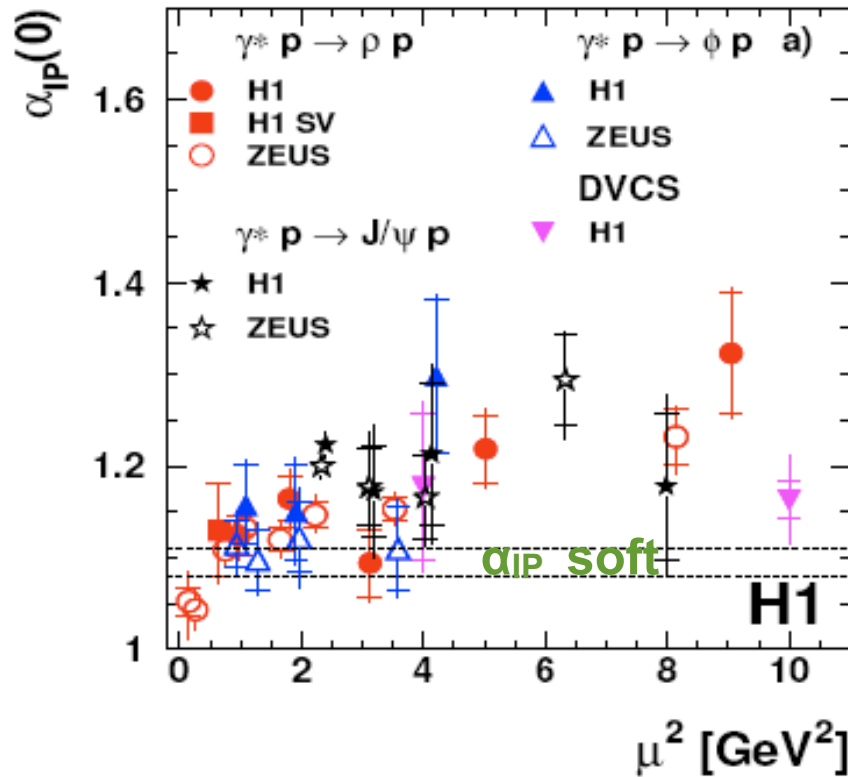
[arXiv:1109.0432v1](https://arxiv.org/abs/1109.0432v1)

Abstract

We show that the supersymmetric extension of the Standard Model modifies the structure of the low lying BFKL discrete pomeron states (DPS) which give a sizable contribution to the gluon structure function in the HERA x and Q^2 region. The comparison of the gluon density, determined within DPS with N=1 SUSY, with data favours a supersymmetry scale of the order of 10 TeV. The DPS method described here could open a new window to the physics beyond the Standard Model.

Backup slides

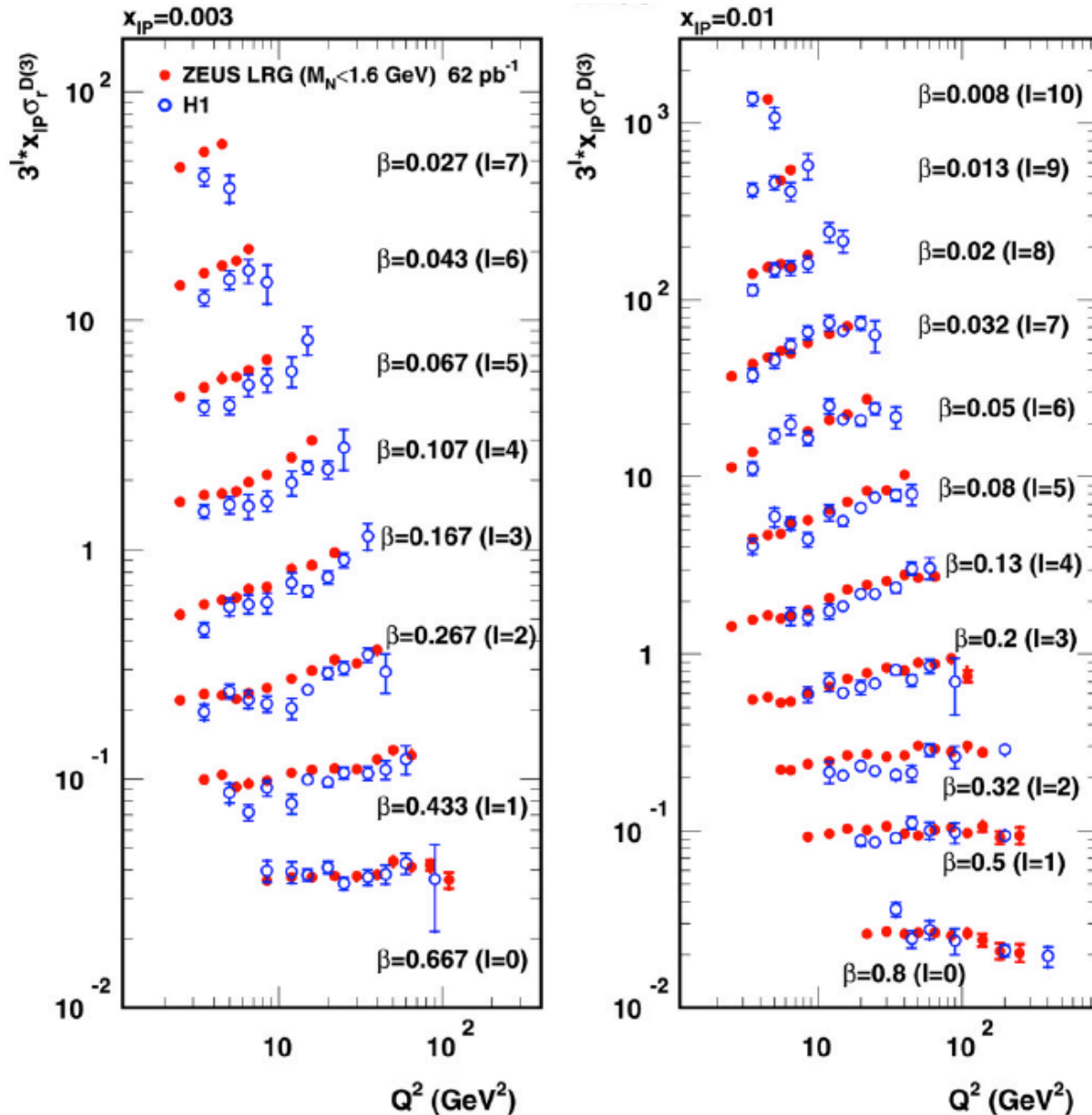
α_{IP} in exclusive VM reactions



J/ψ and ρ show a clear increase of α_{IP} with the increase of scale

(in agreement with the dipole expectations that $\sigma_{\text{qq}} \sim (xg(x, \mu^2))^2$)

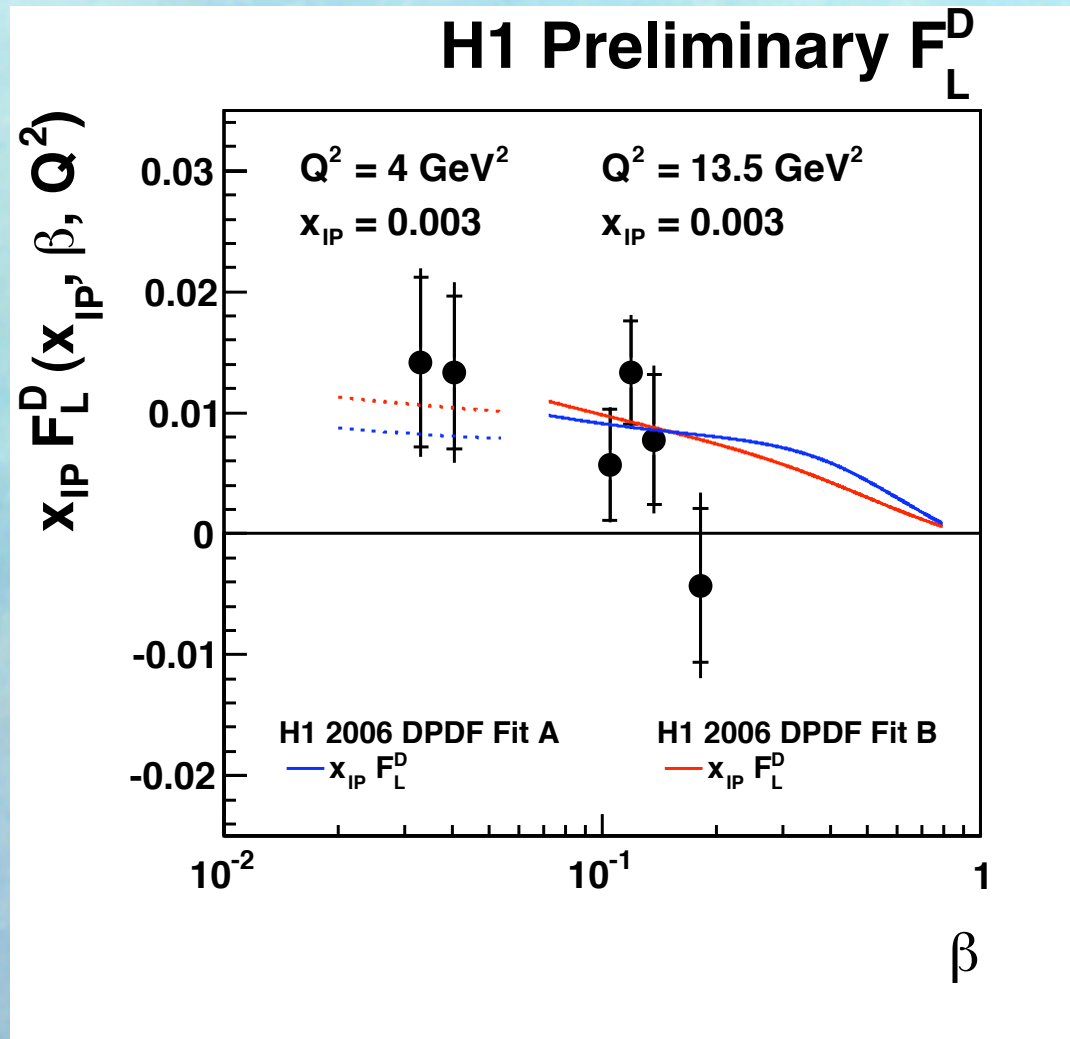
H1-LRG vs ZEUS LRG



general overall agreement

work in progress on understanding systematic differences and on combined H1 and ZEUS inclusive diffraction data

H1 - first measurement of the longitudinal diffractive structure function



possible due to the excellent backward electron measurement in H1